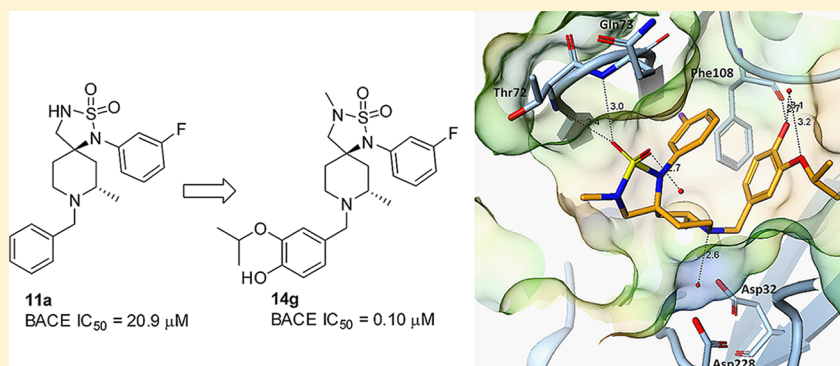


Spirocyclic Sulfamides as β -Secretase 1 (BACE-1) Inhibitors for the Treatment of Alzheimer's Disease: Utilization of Structure Based Drug Design, WaterMap, and CNS Penetration Studies To Identify Centrally Efficacious Inhibitors

Michael A. Brodney,^{*,†} Gabriela Barreiro,[†] Kevin Ogilvie,[†] Eva Hajos-Korcsok,[†] John Murray,[†] Felix Vajdos,[‡] Claude Ambrose,[†] Curt Christoffersen,[†] Katherine Fisher,[†] Lorraine Lanyon,[†] JianHua Liu,[†] Charles E. Nolan,[†] Jane M. Withka,[‡] Kris A. Borzilleri,[‡] Ivan Efremov,[†] Christine E. Oborski,[†] Alison Varghese,[‡] and Brian T. O'Neill[†]

[†]Department of Neuroscience and [‡]Center of Chemistry Innovation and Excellence, Pfizer Worldwide Research and Development, Eastern Point Road, Groton, Connecticut 06340, United States

S Supporting Information



ABSTRACT: β -Secretase 1 (BACE-1) is an attractive therapeutic target for the treatment and prevention of Alzheimer's disease (AD). Herein, we describe the discovery of a novel class of BACE-1 inhibitors represented by sulfamide **14g**, using a medicinal chemistry strategy to optimize central nervous system (CNS) penetration by minimizing hydrogen bond donors (HBDs) and reducing P-glycoprotein (P-gp) mediated efflux. We have also taken advantage of the combination of structure based drug design (SBDD) to guide the optimization of the sulfamide analogues and the in silico tool WaterMap to explain the observed SAR. Compound **14g** is a potent inhibitor of BACE-1 with excellent permeability and a moderate P-gp liability. Administration of **14g** to mice produced a significant, dose-dependent reduction in central $A\beta_{X-40}$ levels at a free drug exposure equivalent to the whole cell IC_{50} (100 nM). Furthermore, studies of the P-gp knockout mouse provided evidence that efflux transporters affected the amount of $A\beta$ lowering versus that observed in wild-type (WT) mouse at an equivalent dose.

INTRODUCTION

Alzheimer's disease (AD), the most common neurodegenerative disorder, is defined clinically by a slowly progressing loss of cognitive function, ultimately leading to dementia and death. AD pathology is characterized by the presence of extracellular plaques in the hippocampal and cortical regions of the brain, accompanied by intraneuronal neurofibrillary tangles and extensive neuronal loss. The primary components of plaques are insoluble aggregates of amyloid- β ($A\beta$) peptides of 38–43 amino acids in length. According to the amyloid hypothesis, increased production and/or decreased clearance and degradation of $A\beta$ initiate a molecular cascade leading to neurodegeneration and AD.^{1,2} $A\beta$ is derived from sequential cleavage of the type I integral membrane protein, amyloid precursor protein (APP), by two proteases, β - and γ -secretase.³

Proteolytic cleavage of APP by the β -site APP-cleaving enzyme (BACE-1) takes place within the endosome at low pH and generates a soluble N-terminal ectodomain of APP (sAPP β) and the C-terminal fragment C99.⁴ Subsequent cleavage of the membrane-bound C99 fragment by γ -secretase liberates the various $A\beta$ isoforms, of which $A\beta_{40}$ and $A\beta_{42}$ are the predominant forms.⁵ In vitro characterization suggests that BACE-1 is the rate-limiting enzyme for the generation of $A\beta$ peptides and therefore an attractive target for the development of AD therapeutics.

Special Issue: Alzheimer's Disease

Received: July 3, 2012

Published: September 17, 2012

Early work on β -secretase inhibitors focused on peptidic transition state mimics that took advantage of lipophilic interactions with binding pockets on the N-terminal (“non-prime”) or C-terminal (“prime”) sides of the scissile bond. Unfortunately, the majority of these inhibitors failed to reduce brain $A\beta$ levels because of poor exposure in the CNS.⁶ In most cases, significant P-gp mediated efflux likely prevented adequate levels of drug from crossing the blood–brain barrier (BBB) because of the high molecular weight, large total polar surface area, and undesirable number of hydrogen bond donors (HBDs) characteristic of these compounds.^{7–10} To identify inhibitors with robust CNS penetration, novel scaffolds with improved properties for a CNS drug candidate were sought.¹¹

In recent years, alternative chemotypes such as acylguanidine, aminothiazine, and aminoimidazole based inhibitors were discovered that bind directly to the catalytic aspartic acids (Asp32 and Asp228) in BACE-1 by displacing the tightly bound catalytic water.^{12–16} Efficient ligand binding requires compensation for the high desolvation costs by binding interactions between the catalytic aspartates and a strongly basic ligand via multiple hydrogen bond interactions. If the tightly bound catalytic water is considered part of the binding site, an indirect ligand–protein contact could occur via a water mediated hydrogen bond to the inhibitor. In this manner, the protein desolvation penalty would be greatly reduced and a less basic inhibitor with fewer H-bond donors could be envisaged. Recent reports in the literature described several classes of BACE-1 inhibitors (1–3) that do not displace the catalytic water but rather make a hydrogen bond via the water to the catalytic aspartates (Figure 1). Of particular interest were a class

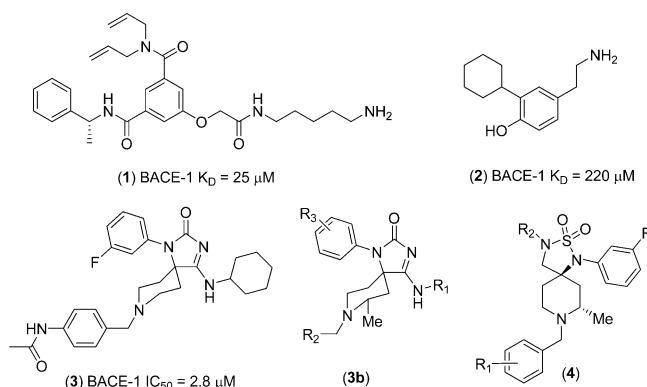


Figure 1. Examples of BACE inhibitors that do not displace catalytic water.

of tyramine derivatives (2) and iminohydantoin spiro-piperidines (3) that were confirmed through X-ray analysis to bind to the active site via a water mediated hydrogen bond with a protonated basic amine.^{17–20} The tyramine derivatives (2) bind to the catalytic aspartates with the protonated primary amine which places the cyclohexyl group in the S3 pocket.²⁰ Key features of the iminohydantoin (3) complex with BACE-1 were a hydrogen bond between the N–H of Gln73 of the protein flap and the carbonyl group of the hydantoin and the arylacetamide binding in the S1 pocket.¹⁷ Inspired by these structures, we designed a series of spirocyclic sulfamides (4) aiming to make further interactions with the protein flap via the sulfone group. Described in this paper is the optimization of a class of spirocyclic sulfamides 4 using a combination of structure based drug design (SBDD) and WaterMap²¹ to guide

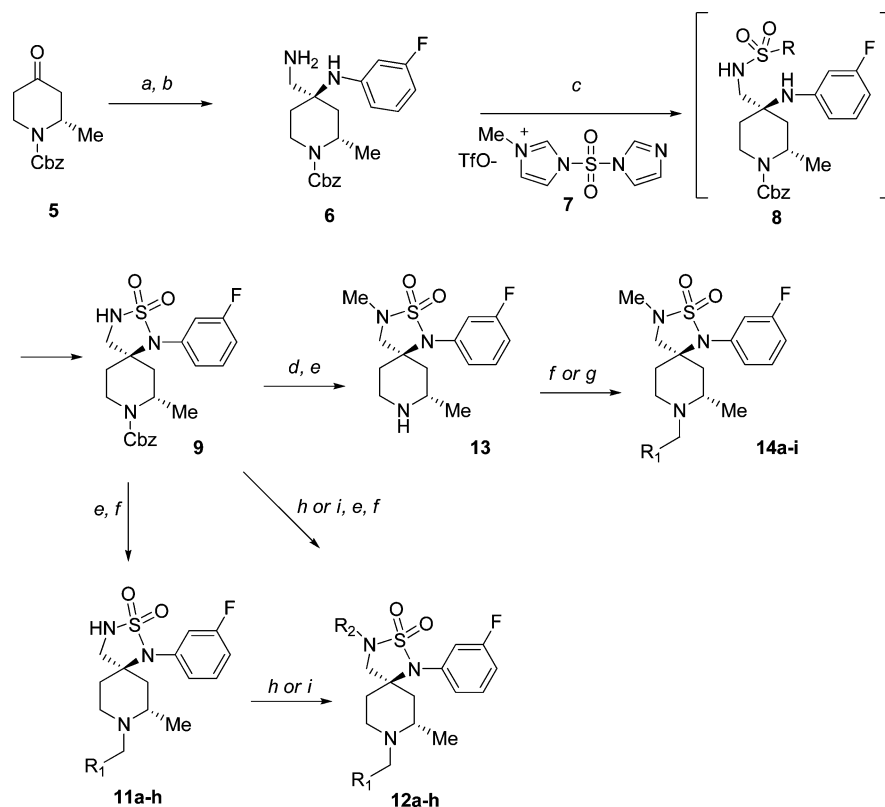
and explain new SAR that ultimately led to the discovery of a potent, selective, and centrally efficacious BACE inhibitor.

CHEMISTRY

The synthesis of spirocyclic sulfamides (4) as represented by analogues 11a–h is illustrated in Scheme 1. The key step in the synthetic route is the cyclization of diamine 6 to generate sulfamide 9. The synthesis of diamine 6 began with a Strecker reaction of chiral piperidinone 5, which proceeded with modest stereoselectivity (3:2) favoring the desired product.^{22–24} Following separation of the diastereomers, the nitrile was reduced to diamine 6 using Raney nickel. Initial attempts to cyclize diamine 6 by treatment with sulfamide/pyridine at 120 °C provided the desired sulfamide 9 in only 6% isolated yield. In order to improve the yield, we sought a more reactive source of the sulfonyl (SO₂) group. Reaction of 6 with sulfur chloride (SO₂Cl₂) was next attempted, but only trace product was observed; the major product was dimerized starting material. Attempts to carry out the ring closure in a two-step process by treatment with sulfamide (NH₂SO₂NH₂) or dimethylsulfamoyl chloride (ClSO₂NMe₂) gave cyclization precursor 8 (where R = NH₂ or NMe₂); however, further attempts to cyclize these intermediates to sulfamide 9 failed to provide the desired material. Following the conditions of Beaudoin, using the triflate salt of mono-*N*-methyl-*N,N'*-sulfuryldiimidazole (7), the ring closure was successfully achieved in 30% yield.²⁵ Further optimization by the dropwise addition of 6 to a solution of triflate salt 7 in acetonitrile decreased side product formation and provided 9 in 44% yield. Conversion of 9 into the desired piperidine analogues 11a–h was accomplished by deprotection of the Cbz group using H₂/Pd(OH)₂ followed by reductive amination with an appropriate benzaldehyde. Further functionalization of the sulfamide 11 at sulfamide nitrogen was accomplished via *N*-alkylation with an appropriate alkyl halide or *N*-arylation using copper(I)-mediated coupling to provide sulfonamides 12a–h.²⁶ Alternatively, the sulfamide 9 was first functionalized using *N*-alkylation or *N*-arylation conditions followed by deprotection and reductive amination to furnish 12a–h. Sulfamide 9 was also alkylated with methyl iodide; removal of the Cbz protecting group provided *N*-methylsulfamide 13. Reductive amination with an appropriate benzaldehyde or alkylation with a benzylic bromide provided piperidine analogues 14a–g.

RESULTS AND DISCUSSION

We began our SAR exploration by varying the substituents on the piperidine nitrogen (R₁, see Table 1). The benzyl analogue 11a was prepared first and showed weak binding activity (IC₅₀ = 20.9 μM) in our BACE-1 cell-free assay (CFA), with a moderate MDR efflux ratio (MDR Er) of 2.5 in an MDR1-transfected MDCK cell line; this suggested the potential for this compound to be a substrate for the P-gp efflux transporter.²⁷ To rapidly expand the SAR, the effect of a wide range of aryl, heteroaryl, and cycloalkyl R₁ substituents was investigated using plate-based synthesis. Alkyl ethers at the ortho or para positions of aryl rings were inactive (IC₅₀ > 300 μM) in the CFA (data not shown), but meta substituents such as ethers (11c–g) improved BACE-1 potency relative to 11a. Within this series of analogues, the isopropyl congener (11d) appeared to be optimal for potency relative to methyl ether (11b), ethyl ether (11c), branched alkyls (11f), or cycloalkyls (11g). Potency was not directly correlated to lipophilicity (clogP) or molecular

Scheme 1^a

^aReagents and conditions: (a) $\text{Zn}(\text{CN})_2$, 3-fluoroaniline, CH_2Cl_2 , 80–90%, then chiral HPLC; (b) Raney Ni, 2 N NH_3 , MeOH, 50–60%; (c) 7, CH_3CN , rt, 44%; (d) NaH, DMF, 0 °C, then MeI, rt, 95%; (e) $\text{Pd}(\text{OH})_2$, 2 N NH_3 , MeOH, H_2 , 50 psi; (f) RCHO , $\text{Cl}(\text{CH}_2)_2\text{Cl}$, AcOH, then $\text{NaBH}(\text{OAc})_3$, rt, 40–80% over two steps; (g) Cs_2CO_3 , DMF, $\text{R}_1\text{CH}_2\text{Br}$, rt, 35–60%; (h) R_2X , CuI, K_2CO_3 , *N,N'*-dimethylethane-1,2-diamine, dioxane, 105 °C, 12–24 h, 30–68%; (i) NaH, DMF, 0 °C then R_2X , rt, 20–93%.

weight (MW). In addition, analogue **11d** showed minimal difference between the cell-free assay ($\text{IC}_{50} = 1.3 \mu\text{M}$) and whole-cell assay (WCA $\text{IC}_{50} = 2.9 \mu\text{M}$), indicating the absence of barriers to cellular penetration. Further profiling for potential P-gp mediated efflux demonstrated that **11d** was a substrate, with $\text{MDR Er} = 3.5$. Replacing the ether group of **11b–g** with a biaryl substituent (**11h**) led to a significant improvement in enzyme inhibition but at the expense of significant P-gp mediated efflux ($\text{MDR Er} = 16$). We postulated that the high predicted P-gp efflux may be due in part to the combination of high molecular weight and the presence of a hydrogen bond donor (HBD) in the sulfamide. Thus, the follow-up strategy to analogues **11a–h** was to reduce efflux from the CNS by capping the N–H sulfamide to reduce the HBD count.

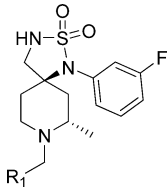
To investigate the sulfamide substituent (R_2), a series of alkyl- and heteroaryl-substituted compounds were prepared and evaluated in the CFA and WCA and for efflux potential (Table 2). The methyl analogue **12a** showed comparable cellular potency with reduced P-gp mediated efflux, compared to the N–H analogue **11d** ($\text{MDR Er} = 1.7$ vs 3.8). Attempts to improve potency by replacing the methyl of sulfamide **12a** with ethyl (**12b**) or isopropyl (**12c**) resulted in loss of ligand efficiency (LE) and were not further pursued. We next investigated heterocyclic R_2 substituents, which we anticipated would make unique interactions with the protein flap and potentially increase potency. To this end, a set of heteroaryls including pyridines **12d–e**, pyrimidine **12f**, thiazole **12g**, and oxazole **12h** were prepared (see Chemistry section). In general, the potency was not significantly improved by varying the

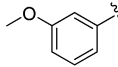
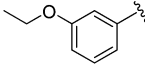
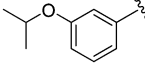
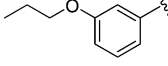
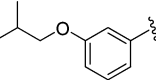
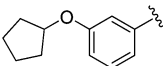
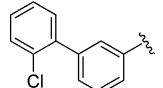
heterocycle off the sulfonamide (R_2). Relative to the alkyl analogues **12a–c**, the heterocyclic variants also suffered from reduced passive permeability in the RRCK cell line.²⁸ Despite the increase in MW for analogues **12b–h** relative to **12a**, the projected P-gp efflux values remained low underscoring the importance of reducing the number of HBDs when designing in a higher range of MW (Table 2).¹¹

Relative to most peptidomimetic BACE-1 inhibitors, compound **12a** possesses unique physicochemical properties. The compound lacks a hydrogen bond donor, has moderate TPSA of 69, and has a clogP of 3.9. This physicochemical property space represents a significant improvement over classical BACE-1 inhibitors.^{6–9} To further understand the brain penetration of this series, a mouse CNS pharmacokinetic study was conducted with analogues **11d** and **12a** (Table 4).²⁹ Both analogues showed good brain to plasma ratio (**11d**, 0.67; **12a**, 0.97); however, compound **12a** also displayed favorable unbound brain to unbound plasma ratios ($C_{u,b}/C_{u,p}$ of 0.67 vs 0.2 for **11d**), suggesting that no efflux transporters were limiting access to the central compartment.

On the basis of the attractive binding, selectivity, and CNS penetration, the structure of **12a** bound to BACE-1 was determined by X-ray crystallography (Figure 2). The compound adopts a folded conformation that places the fluorophenyl and isopropoxyphenyl rings in proximity to one another, presumably stabilized by π – π stacking interactions and/or hydrophobic collapse (see Supporting Information Table 1 for refinement statistics). The protonated nitrogen of the piperidine directly hydrogen-bonds to the catalytic water

Table 1. In Vitro Pharmacology, MDR Efflux Ratio, and Physicochemical Properties for 11a–h



Compd	R ₁	CFA IC ₅₀ (μM) ^a	WCA IC ₅₀ (μM) ^b	MDR Er ^c	clogP/MW
11a		20.9	ND	2.5	4.06/389
11b		99.3	ND	2.4	3.98/420
11c		9.5	3.3	3.4	4.51/434
11d		1.3	2.9	3.8	4.82/448
11e		23.1	ND	3.1	5.04/448
11f		11.2	7.1	4.7	5.44/462
11g		11.0	5.3	5.0	5.45/474
11h		1.7	0.71	16.1	6.41/500

^aIC₅₀ values obtained from BACE-1 cell free assay (CFA). ^bIC₅₀ values obtained from BACE-1 whole cell assay (WCA); ND = not determined. ^cMDR efflux ratio (MDR Er) from MDR1-transfected MDCK line.

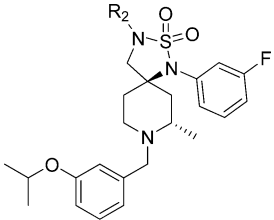
situated between the catalytic aspartates Asp32 and Asp228 in a manner similar to that reported in the literature for compounds **2** and **3**.^{17,20} One sulfamide oxygen accepts two hydrogen bonds, one from the backbone N–H of Thr72 and the other from the backbone N–H of Gln73. The methyl group of the spiro-piperidine inserts into a small cleft at the back of the binding pocket. The fluorophenyl ring occupies what we termed the S1a site, as this pocket is primarily an extension of the S1 pocket. The isopropoxyphenyl group is situated squarely in the S1 pocket, with the isopropoxy group extending into the S3 pocket. Several waters, both crystallographic and modeled, are displaced by the isopropoxy group.

Although crystal structures provide information regarding steric and electrostatic factors, some aspects of ligand SAR cannot be accounted for, so additional computational analysis is required for a comprehensive explanation of the available SAR. One such method, applied in this work to help explain the SAR shown in Table 1, is the use of WaterMap.²¹ This method computes the free energy of hydration (ΔG_{hyd}) for binding site waters, that is, the energy difference associated with the

displacement of water molecules from the protein binding site into bulk solution.³⁰ WaterMap is well-suited to the analysis of congeneric molecules where small structural modifications can result in changes in activity.

The ΔG_{hyd} was computed for the crystal structure of compound **12a** as described in the Computational Details section. The hydration sites can be seen in Figure 3. Stable hydration sites ($\Delta G_{\text{hyd}} < 0.0$ kcal/mol) with respect to bulk water are shown in green, unstable hydration sites ($\Delta G_{\text{hyd}} > +1.0$ kcal/mol) in red, and those that are moderately unstable ($0.0 < \Delta G_{\text{hyd}} < +1.0$ kcal/mol) in yellow. These ranges were assigned based on the ΔG_{hyd} values obtained for the water molecules in the BACE binding site. The core of the spiro-piperidine analogues overlaps with eight hydration sites, all of which are unfavorable with free energies ranging from +0.5 to +5 kcal/mol. Hydration site 2, one of the most unstable of all 22 hydration sites computed in the BACE-1 binding pocket, showed a ΔG_{hyd} of +4.94 kcal/mol and overlaps with the fluorine atom of the phenyl ring. All the remaining

Table 2. In Vitro Pharmacology, MDR Efflux Ratio, and Passive Permeability for 12a–h



Cmpd	R ₂	CFA IC ₅₀ (μM) ^a	WCA IC ₅₀ (μM) ^b	MDR Er ^c	RRCK (×10 ⁻⁶ cm/s) ^d
12a	Me	2.4	1.8	1.7	7.48
12b	Et	1.7	ND	2.7	17.5
12c	iPr	2.3	1.4	2.4	7.96
12d		4.0	3.0	1.0	10
12e		3.1	3.6	1.9	2.24
12f		1.5	2.5	2.6	3.37
12g		2.2	4.1	>4.4	0.53
12h		1.7	>10.2	2.1	0.83

^aIC₅₀ values obtained from BACE-1 CFA. ^bIC₅₀ values obtained from BACE-1 WCA; ND = not determined. ^cMDR efflux ratio (MDR Er) from MDR1-transfected MDCK line. ^dRRCK cells with low transporter activity were isolated from Madin–Darby canine kidney cells and were used to estimate intrinsic absorptive permeability.²⁸

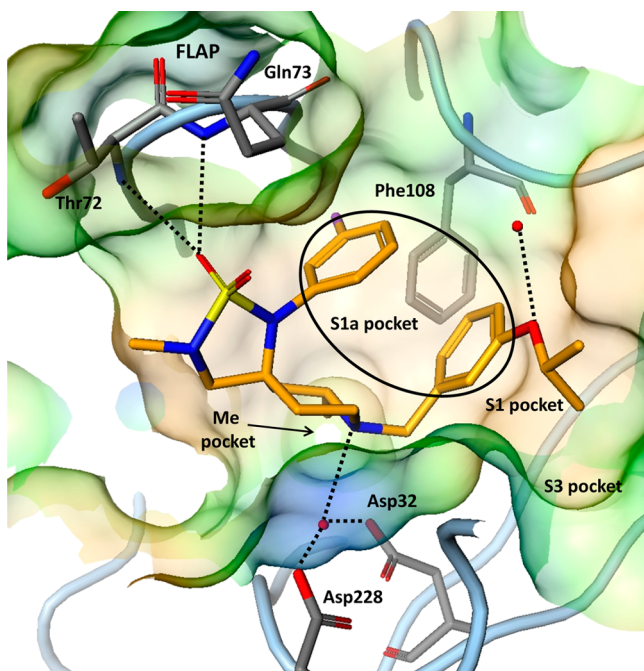


Figure 2. X-ray structure of compound 12a bound to BACE-1.

hydration sites (1,3–8) display ΔG_{hyd} values between +0.5 and +2.5 kcal/mol.

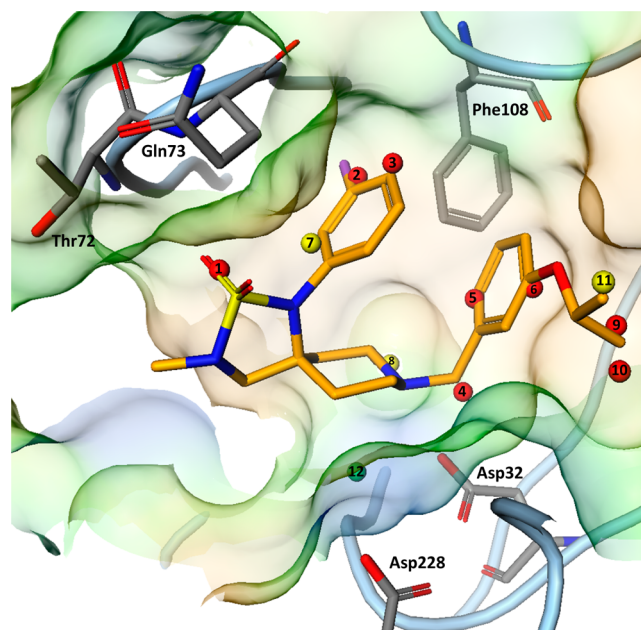


Figure 3. X-ray crystal structure and overlapping hydration sites for compound 12a bound to BACE-1.

As shown in Table 1, the unsubstituted phenyl compound 11a has an IC₅₀ of 20.9 μM. The addition of the isopropoxy (11d) and biaryl (11h) groups resulted in almost 20-fold

increase in potency (IC_{50} of 1.3 and 1.7 μM , respectively). This can be understood by considering the displacement of water from hydration sites 9, 10, and 11 with ΔG_{hyd} of +5.7, +3.2, and +0.8 kcal/mol, respectively. Hydration site 9 showed the second most unfavorable free energy of all hydration sites computed. Compound **11d** displays a binding mode very similar to the one observed in the X-ray structure for compound **12a**, with the isopropoxy group overlapping very well with the three unfavorable hydration sites. A similar binding mode is predicted by modeling of the biaryl derivative **11h**. The significant increase in potency seen for compounds **11d** and **11h** may be attributable to the free energy gain from release of these three waters into bulk solution. The reduced affinity for the methoxy analogue (**11b**) is probably related to its inability to displace water from these unfavorable hydration sites (9, 10, and 11). A more flexible alkoxy side chain present in compounds **11e** and **11f** and a more rigidified one present in compound **11g** might be preventing an ideal overlap with the same unstable water molecules and could be responsible for the weak potency observed for these compounds. Compound **11b** may also suffer an increased desolvation penalty when compared to compound **11a** caused by the presence of the ether oxygen. Although the same argument can be extended to the ether analogues in Table 1, the free energy gain from the liberation of waters 9, 10, and 11 largely offsets the increased desolvation penalty for the analogues able to displace the unstable hydration sites.

The important role that binding-site waters play in the binding affinity differences for the compounds in Table 1 can be further supported by the good correlation ($R^2 = 0.82$) between the experimental data and the WaterMap free energy liberation (ΔG_{WM}) (Figure 4). ΔG_{WM} estimates the free energy

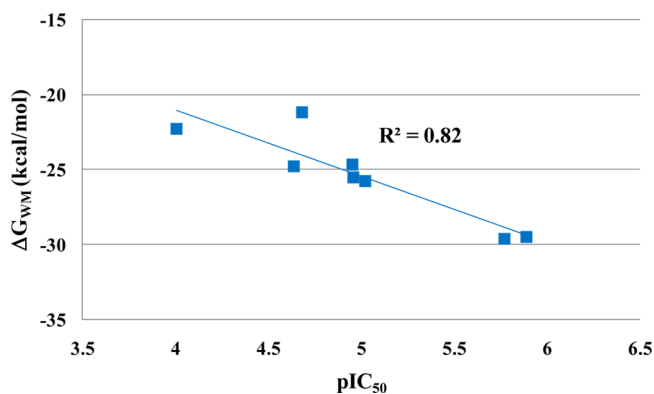


Figure 4. Correlation between the experimental activities and the WaterMap free energy liberation of binding site waters for spiro-piperidines analogues in Table 1 (see Supporting Information Table 2 for the ΔG_{WM} , ΔH_{WM} and $-T\Delta S_{\text{WM}}$ values).

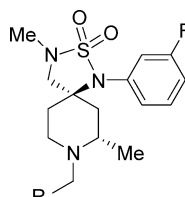
gained when a ligand that is suitably complementary to the binding site displaces the waters therein into bulk solution.²⁸ Therefore, the R_1 groups that displace the most unfavorable binding-site waters result in the most potent compounds. The WaterMap results can also help rationalize, from protein-hydration observations, the flat SAR observed for compounds in Table 2. First, the waters in that region of the binding site are not particularly unfavorable ($0.0 < \Delta G < +1.0$ kcal/mol), as that site is somewhat more solvent-exposed. Second, the analogues are similar in size, except for **12a**, and displace essentially the same water molecules. Also, the R_2 substituents

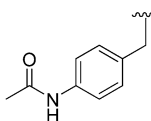
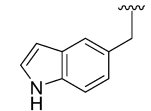
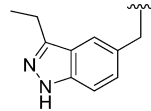
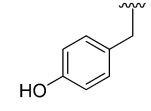
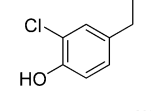
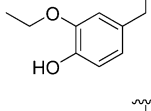
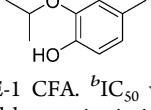
examined are not likely differentiated on the basis of formation of specific H-bonds with the protein.

The discovery of **12a** indicated that the spirocyclic sulfamide template was a viable starting point for further optimization of potency and ADME properties. Analysis of the X-ray structure of **12a** suggested that interactions with the backbone carbonyl of residue Phe108 could potentially provide improved potency. An extensive SAR effort was undertaken to replace the benzyl group of **12a** with an aromatic group lacking additional HBDs; however, we were unable to identify alternative analogues with improved binding potency and ADME properties relative to **12a**. Despite the inherent risk of adding back a HBD into the R_1 group due to the potential for increased P-gp efflux, we synthesized and profiled a series of analogues containing an acetamide, phenol, or N-H heterocycle (Table 3). Installation of an acetamide in the para position of the benzyl group in (**14a**) resulted in reduced potency relative to **12a** and significant P-gp mediated efflux (MDR Er = 7.4). Indole **14b** indicated that heteroaromatics in the S1 pocket gave reduced P-gp efflux but additional substituents off the heteroaryl ring would be required for improved binding activity. To this end, ethylindazole **14c** was designed to make an interaction with Phe108 and displace unstable water molecules in hydration sites 9–11 (Figure 3); this yielded improved cellular potency relative to **14b**. We next postulated that a phenol might efficiently interact with Phe108, which proved to be the case (Table 3). Isothermal titration calorimetry (ITC) data for compound **12a** showed a free energy of binding of -8.15 kcal/mol with an enthalpic contribution of -10.3 kcal/mol. In the case of the unsubstituted phenol analogue (**14d**), a free energy of binding of -8.6 kcal/mol with an enthalpic contribution of -10.7 kcal/mol was obtained suggesting that the phenol OH is engaged in favorable interactions with the protein. The entropic contributions for **12a** and **14d** were essentially equivalent. Inspired by this observation and the earlier ether SAR (Table 1), a series of disubstituted analogues **14e–g** were designed and synthesized (see Chemistry section). As was previously observed (Table 1), the isopropyl analogue **14g** provided superior potency relative to a range of other ethers including the ethyl ether **14f** as well as the chloro analogue **14e**. Compound **14g** exhibited a ~ 10 -fold improvement in free energy of binding (-9.88 kcal/mol) relative to **12a**. In addition, **14g** showed improved binding kinetics, with a measurable off rate of 0.034 (1/s) compared with the equilibrium binding for **14d** as measured by surface plasmon resonance (SPR) techniques. Interestingly, analogues **14e–g** showed reduced P-gp mediated efflux relative to phenol **14d**. We speculated that an ortho alkoxy substituted phenol such as analogues **14e–g** may engage in intermolecular hydrogen bonding, effectively blocking recognition from the P-gp efflux transporter.^{31,32} Analogue **14g** also exhibited a superior balance of microsomal stability and MDR Er (3.4) relative to other analogues. The structure of isopropoxyphenol (**14g**) bound to BACE-1 is depicted in Figure 5 (see Supporting Information Table 1 for refinement statistics). The structure is essentially identical to that of the parent compound **12a**, with the exception that the phenolic OH is clearly donating a hydrogen bond to the backbone carbonyl of Phe108.

To further understand the in vitro selectivity profile of compounds **12a** and **14g**, screening against the related aspartyl protease cathepsin D (CatD) was initiated. At doses up to 100 μM , compounds **12a** and **14g** showed no inhibition of CatD. In addition, compound **14g** was screened in a broad pharmaco-

Table 3. In Vitro Pharmacology, MDR Efflux Ratio, and Microsomal Stability for 14a–g



Compd	R ₁	CFA IC ₅₀ (μM) ^a	WCA IC ₅₀ (μM) ^b	MDR Er ^c	<i>h</i> -CLint, scaled (mL/min/kg) ^d
14a		6.4	7.4	7.4	>300
14b		6.1	0.77	2.4	175
14c		1.1	0.29	6.5	74.2
14d		0.27	0.24	4.3	152
14e		1.6	0.35	2.2	173
14f		1.2	1.6	2.3	79.9
14g		0.10	0.10	3.4	73.9

^aIC₅₀ values obtained from BACE-1 CFA. ^bIC₅₀ values obtained from BACE-1 WCA. ^cPredicted MDR efflux ratio (MDR Er) from MDR1-transfected MDCK line. ^dPredicted human intrinsic clearance, scaled (*h*-CLint, scaled) from human liver microsomal stability assay.

logical panel (Cerep) and exhibited greater than 100-fold selectivity versus other receptors and enzymes with the exception of L-type Ca²⁺ channel activity (see Supporting Information Table 3).

Analogous to compounds **11d** and **12a**, isopropoxyphenol **14g** underwent brain penetration studies in the mouse with C_{u,b}/C_{u,p} = 0.27 (Table 4). The C_{u,b}/C_{u,p} ratio for **14g** showed asymmetry between unbound drug concentrations in the plasma and brain compartment, suggesting involvement of an efflux transporter. The MDR Er data support the conclusion that P-gp is involved in the observed asymmetric distribution of **14g** in plasma and brain. Despite the reduced brain penetration of **14g** relative to **12a**, the higher free fraction (f_u plasma), excellent potency, and selectivity of **14g** suggested this was an excellent tool to advance our understanding of the PK–PD relationship between unbound drug concentrations and Aβ reductions in relevant peripheral and central compartments

(plasma, brain, CSF). At 3 h following subcutaneous administration of a single dose of **14g** to wild-type FVB mice (WT), significant dose-dependent reductions were observed in both brain and CSF Aβ₄₀ levels at the two highest doses (100 and 300 mg/kg; Figure 6a and Figure 6c). The changes in Aβ₄₂ paralleled those of Aβ₄₀ in the brain, with statistically significant lowering reached at the 30–300 mg/kg doses (Figure 6b). The compound also elicited a robust decrease in plasma Aβ₄₀ (average 55%) compared to vehicle control across the doses examined (Figure 6d). The non-dose-dependent changes in the plasma suggest that maximum reductions likely have been achieved in this compartment at all doses tested, consistent with the 55% Aβ₄₀ reduction reported in the plasma of BACE-1(–/–) vs BACE-1(+ / +) mice.³³

In vivo efficacy of **14g** was also tested in P-gp knockout mice, an animal model that has functional deficiency at the blood–brain barrier due to disruption of the MDR1a efflux

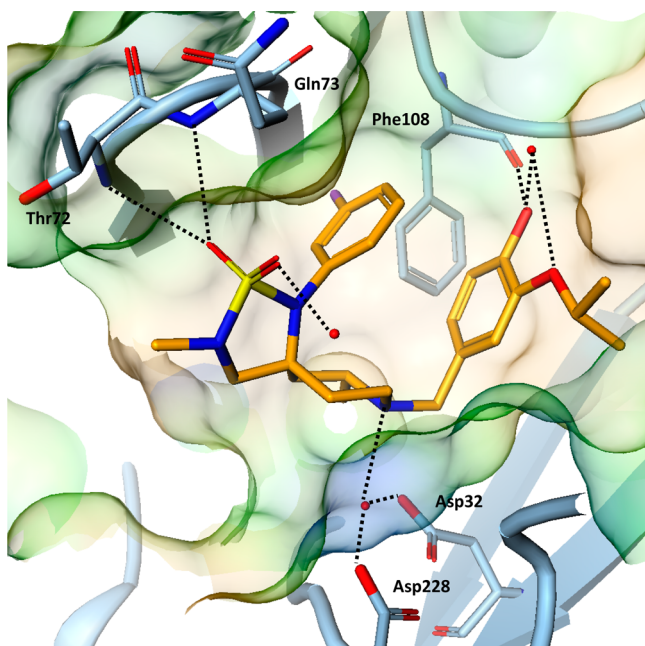


Figure 5. X-ray structure of compound **14g** bound to BACE-1.

Table 4. In Vitro and in Vivo PK Properties of Representative Compounds

PK properties	11d	12a	14g
MDCK AB (10^{-6} cm/s) ^a	10.2	7.5	17.6
MDR BA/AB ^b	3.8	1.7	3.3
in vitro <i>h</i> -CL _h ($\text{mL min}^{-1} \text{kg}^{-1}$) ^c	>19	>19	15.4
in vitro <i>r</i> -CL _h ($\text{mL min}^{-1} \text{kg}^{-1}$) ^d	>65.5	>65.5	59.7
<i>B/P</i> (mouse) ^e	0.67	0.97	0.35
<i>F_u</i> (plasma) ^f	0.041	0.036	0.17
<i>F_u</i> (brain) ^f	0.018	0.024	0.12
<i>C_{ub}/C_{up}</i>	0.22	0.65	0.27

^aMS-based quantification of the basal/apical transfer rate of a test compound at 2 μM across contiguous monolayers from MDCK (Madin–Darby canine kidney) cells. ^bRatio from the MS-based quantification of apical/basal and basal/apical transfer rates of a test compound at 2 μM across contiguous monolayers from MDR1-transfected MDCK cells. ^cHepatic clearance predicted from in vitro human microsomal stability study. ^dHepatic clearance predicted from in vitro rat microsomal stability study. ^eDetermined from plasma and brain exposures in mice 60 min after 10 mg/kg subcutaneous dosing. ^fDetermined from equilibrium dialysis.

transporter.³⁴ At 3 h after sc administration of **14g**, robust brain $A\beta_{40}$ lowering was achieved even at low doses, with statistically significant effects starting at the 3 mg/kg sc dose (Figure 6e). At the 10–300 mg/kg dose range, brain drug exposures were about 7- to 12-fold higher in P-gp KO mice compared to the WT strain (see Supporting Information Table 4). Importantly, brain $A\beta$ -lowering efficacy of **14g** shows a consistent relationship with brain exposures across the two mouse strains (Figure 6f), with significant $A\beta$ reductions associated with a range of drug concentrations. These data also suggest that maximum $A\beta$ reductions are about 65% of vehicle control under the present experimental conditions, and no further $A\beta$ lowering can be achieved despite robust increases in brain exposures. The reason for this residual $A\beta$ is not clear, but could be due, at least in part, to the limitations of single time-point data collection in the present study.

CONCLUSION

Described herein is the identification and optimization of a novel series of spirocyclic sulfamide BACE-1 inhibitors that bind to the catalytic aspartic acids via water mediated hydrogen bond. A combination of SBDD and computational modeling using WaterMap guided the rational design of new analogues and explained the obtained SAR. Excellent in vitro potency was achieved in the series by combining a substituent in the S3 pocket with a phenol of the inhibitor, resulting in favorable interactions with the protein. Improved brain penetration relative to classical BACE-1 inhibitors was achieved by reducing the number of hydrogen bonds, lipophilicity, and molecular weight. Despite the presence of a HBD and modest predicted P-gp efflux, analogue **14g** achieved unbound drug concentrations in brain well above the cell free or whole cell binding affinities. Compound **14g** displays key characteristics of a BACE-1 inhibitor in vivo, significantly reducing β -cleavage of APP and $A\beta$ production in brain, plasma, and CSF in WT mice after an acute dose. The $C_{u,b}/C_{u,p}$ ratio for **14g** in WT mice coupled with the difference in doses required for $A\beta$ lowering in the P-gp KO relative to WT mice suggests that this compound is a substrate for the Pgp transporter. Future effort will focus on identification of BACE-1 inhibitors with reduced asymmetry between the central and peripheral compartments to optimize the therapeutic index.

EXPERIMENTAL SECTION

Biology. BACE-1 Enzyme Cell-Free Assay (CFA). BACE-1 activity was measured using a polyclonal antibody, p1007 (Pfizer), that specifically recognizes the C-terminus of APP_{695Swe} created after cleavage by BACE-1. To generate p1007, rabbits were immunized with the peptide NH₂-EISEVNL-COOH conjugated to keyhole limpet hemacyanin. Concentrated conditioned medium from cells secreting human recombinant soluble BACE-1 was titrated to provide a source of BACE-1 enzyme. The reaction is initiated by the addition of soluble BACE-1 enzyme to a mixture containing 0.05 M sodium acetate (pH 4.5), compound inhibitor, 2% DMSO, and 3 μM APP substrate (K(biotin)RGLTTRPGSGLTNIKTEEISEVNLDAEFRHDSGA, American Peptide). The reaction is incubated at 37 °C for 1 h and quenched by the addition of an equivalent volume of 0.1 M Tris, pH 8.0. Cleaved product is measured via an ELISA with streptavidin-coated plates (Greiner Bio-One), using p1007 reporter antibody (Pfizer) and anti-rabbit horseradish peroxidase (GE Healthcare, U.K.).

sAPP β Whole Cell Assay (WCA). sAPP β , the primary cleavage product of BACE-1, was determined in H4 human neuroglioma cells overexpressing the wild-type human APP₆₉₅. Cells were treated for 18 h with compound in a final concentration of 1% DMSO. sAPP β levels were measured by ELISA with a capture APP N-terminal antibody (Affinity BioReagents, OMA1-03132), wild-type sAPP β -specific reporter antibody p192 (Elan), and tertiary anti-rabbit-HRP (GE Healthcare). The colorimetric reaction was read by an EnVision (Perkin-Elmer) plate reader.

Animals and in Vivo Protocols. All animal procedures were approved by the Institutional Animal Care and Use Committee and were compliant with animal welfare act regulations. Female FVB/N and male P-glycoprotein knockout (P-gp KO) mice (Taconic, Germantown, NY) aged 2–4 months received a single subcutaneous injection of test compound or vehicle (20% DMSO, 20% ethanol in polyethylene glycol), $N = 5$ –6 mice/treatment group. At 3 h following dosing, animals were euthanized with CO₂, and brain, CSF, and blood samples were collected for measurement of $A\beta$ and drug concentrations.

β -Amyloid ELISA. Sample preparation and assay protocols for determination of $A\beta_{40}$ and $A\beta_{42}$ were as described previously.³⁵ Briefly, brains were homogenized in 9 volumes of 5 M guanidine HCl/50 mM Tris-HCl (pH 8.0), extracted for 3 h, and centrifuged at

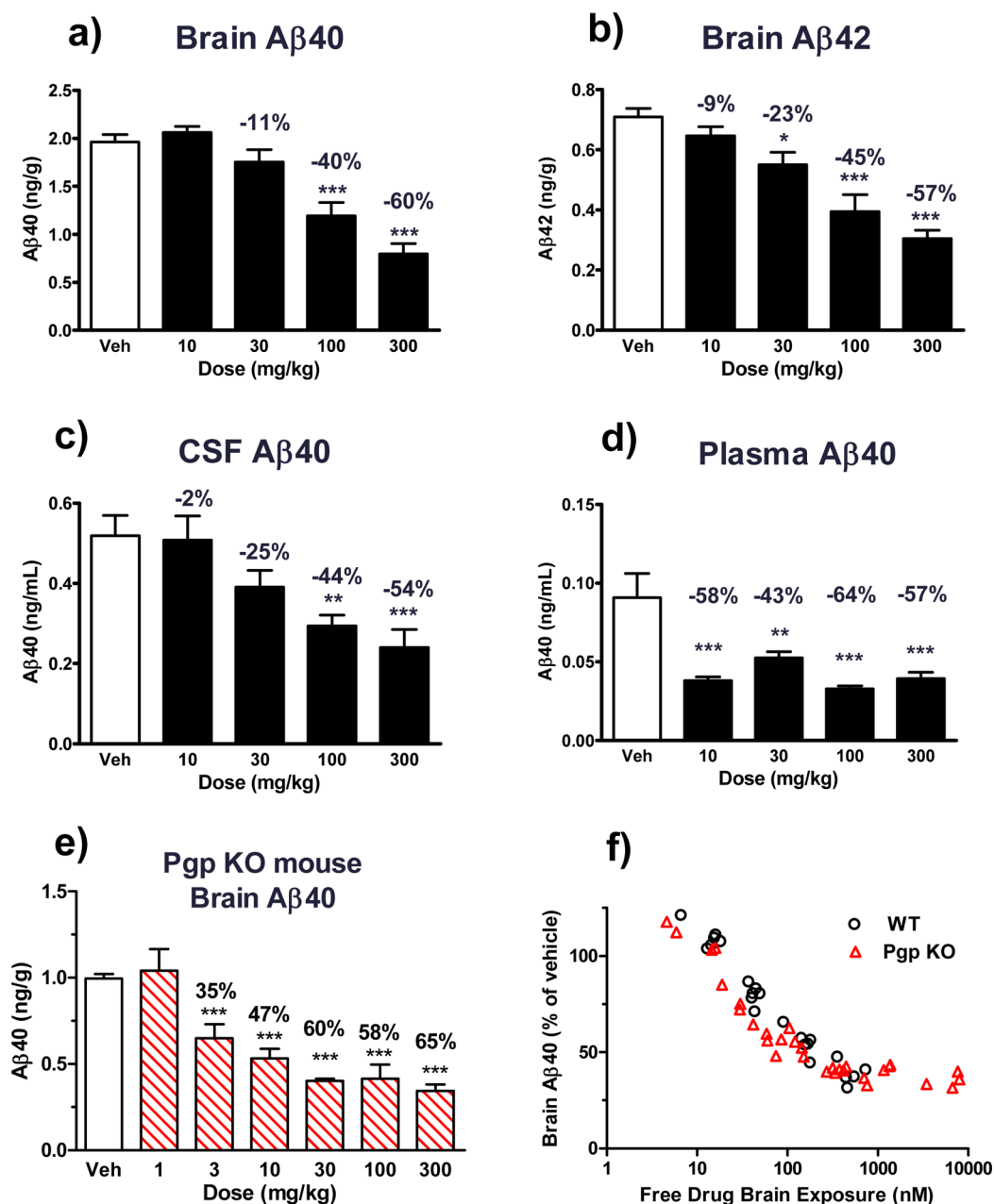


Figure 6. Effect of 14g on Aβ peptide levels in mice at 3 h following acute sc administration. Brain Aβ40 (a), brain Aβ42 (b), CSF Aβ40 (c), and plasma Aβ40 (d) were determined in wild-type (FVB/N) mice, $N = 5-6$ per treatment group by ELISA. Brain Aβ40 lowering was measured in P-gp KO mice using the same experimental conditions for (e) brain exposure–response relationship in WT and P-gp KO mice (f). Statistical analysis was conducted using one-way ANOVA, post hoc Dunnett's test: (*) $p < 0.05$, (**) $p < 0.01$, (***) $p < 0.001$ vs vehicle.

135000g. Aliquots (200 μ L) were analyzed for Aβ40 by a standard Delfia immunoassay using 4 μ g/mL monoclonal antibody 1219 (Rinat, Pfizer) for capture and 0.2 μ g/mL biotinylated 4G8 antibody (Covance) for detection. Fluorescence of the Delfia europium label was measured by an EnVision reader.

Measurement of Fractions Unbound in Brain. The unbound fraction of each compound was determined in brain tissue homogenate using a 96-well equilibrium dialysis method as described by Kalvass et al.²⁹ with the following exceptions. Brain homogenates were prepared from freshly harvested rat brains following dilution with a 4-fold volume of phosphate buffer and spiked with 1 μ M compound. The homogenates were dialyzed against an equal volume (150 μ L) of phosphate buffer at 37 °C for 6 h. Following the incubation, equal volumes (50 μ L) of brain homogenate and buffer samples were collected and mixed with 50 μ L of buffer or control homogenate, respectively, for preparation of mixed matrix samples. All samples were

then precipitated with internal standard in acetonitrile (200 μ L), vortexed, and centrifuged. Supernatants were analyzed using an LC–MS/MS assay. A dilution factor of 5 was applied to the calculation of brain fraction unbound.

X-ray and Biophysics. Crystallization of BACE. Crystals of BACE were prepared as previously described.³⁶ Briefly, recombinant BACE lacking the prosegment was concentrated to 10–13 mg/mL in 0.1 M sodium borate, pH 8.5. Crystallization was done by the vapor diffusion method, using 2 μ L of protein solution and 2 μ L of reservoir solution (30% PEG 200, 0.1 M sodium acetate, pH 5.2–5.4). Drops were microseeded 24 h after setup with 0.3–0.5 μ L of seed stock made from a previously grown BACE-1 crystal. Crystals generally grew to $\sim 0.1 \times 0.1 \times 0.05$ mm³ in 2 weeks. The crystal form is C222₁, with a single molecule of BACE-1 in the asymmetric unit, and diffracts to high resolution ($d_{\min} < 2.0$ Å) with typical X-ray exposure times.

Soaking of Crystals. Soaking solutions were made by diluting the concentrated stock compound mixtures 1:10 with 30% PEG 200 and 0.1 M sodium acetate, pH 5.2. Crystals were transferred individually from their mother drops to a 5 μ L drop of soaking solution and allowed to equilibrate at 21 °C for ~24 h. Following this equilibration, crystals were flash cooled for data collection by harvesting in rayon loops and plunging directly into liquid nitrogen.

Data Collection. X-ray diffraction data were collected in house on a Rigaku MicroMax007HF X-ray generator outfitted with a RaxisIV++ image plate detector. For each crystal a total of 120° of data were collected in 0.5° oscillations, generally yielding ~100% complete data coverage at 4–5 \times redundancy for accurate scaling and outlier rejection. Data processing was performed using D*TREK³⁷ for compound 12a or XDS³⁸ for compound 14g. All data manipulations were performed using the CCP4 suite of programs,³⁹ care being taken to preserve the R_{free} test set for each data set.

Structure Solution. Structures were determined by rigid body refinement using the program REFMAC.⁴⁰ The initial model was a 1.5 Å crystal structure of apo BACE-1 that was solved as part of an ongoing structure-based drug design effort. As we expected conformational variability in the “flap” region of BACE, residues 68–75 were excised from the model prior to refinement to minimize difficulty in interpretation of the $mF_o - dF_c$ σ A-weighted difference maps. Binding of compounds to the BACE-1 active site was assessed by visual inspection of the resulting difference maps using the program COOT.⁴¹ Final refinement was done using AUTOBUSTER.⁴² Refinement statistics are reported in Supporting Information Table 3.

Isothermal Titration Calorimetry. Isothermal titration calorimetry (ITC) experiments were performed using a VP-ITC calorimetric system from MicroCal Inc. Data collection, analysis, and plotting were performed using a Windows-based software package (Origin, version 7.0) supplied by Microcal. All titrations were performed by adding titrant in steps of 8 μ L and were conducted at a constant temperature of 25 °C. All solutions contained within the calorimetric cell and injector syringe were prepared in the same buffer: 50 mM sodium acetate, pH 5.0, 50 mM NaCl, 0.02% sodium azide, and 0.5% DMSO. To assess binding of the compounds to BACE, 10 μ M protein was titrated with 100 μ M compound contained in the injector syringe. All solutions were properly degassed to prevent bubble formation in the calorimetric cell during stirring. The heat evolved upon each injection of compound was obtained from the integral of the calorimetric signal. The heat of dilution was subtracted from the heat of reaction to obtain the heat associated with binding of a ligand to the protein in the cell. Nonlinear regression of the data provided the enthalpy change (ΔH) and association constant (K_a) $1/K_d$.

Surface Plasmon Resonance (SPR) Experiments. Experiments were performed on a Biacore 3000 instrument (GE Healthcare). BACE-1 was immobilized on a CM5 biosensor surface to levels ranging from 4000 to 5000 RU using standard amine coupling procedures. Compound binding experiments were performed in 50 mM sodium acetate, pH 5.0, 150 mM NaCl, 0.05% P20, and 3% DMSO at 25 °C. A series of various compound concentrations were injected over the BACE surface (flow rate 50 μ L/min, contact time 100 s, dissociation time 600 s). Binding responses were processed using Scrubber 2 (BioLogic Software, Inc.) to zero, x -align, double-reference, and correct for excluded volume effects in the data. Scrubber 2 was also used to obtain affinity from steady-state equilibrium data. Kinetic parameters were obtained from global fits of the data to a simple 1:1 interaction model using Biaeval (GE Healthcare).

Chemistry. General Methods. Solvents and reagents were of reagent grade and were used as supplied by the manufacturer. All reactions were run under a N_2 atmosphere. Organic extracts were routinely dried over anhydrous Na_2SO_4 . Concentration refers to rotary evaporation under reduced pressure. Chromatography refers to flash chromatography using disposable RediSepR₄ 4–120 g silica columns or Biotage disposable columns on a CombiFlash Companion or Biotage Horizon automatic purification system. Microwave reactions were carried out in a SmithCreator microwave reactor from Personal Chemistry. Purification by mass-triggered HPLC was carried out using Waters XTerra PrepMS C₁₈ columns, 5 μ m, 30 mm \times 100 mm.

Compounds were presalted as TFA salts and diluted with 1 mL of dimethylsulfoxide. Samples were purified by mass triggered collection using a mobile phase of 0.1% trifluoroacetic acid in water and acetonitrile with a starting gradient of 100% aqueous to 100% acetonitrile over 10 min at a flow rate of 20 mL/min. Elemental analyses were performed by QTI, Whitehouse, NJ. All target compounds were analyzed using ultrahigh performance liquid chromatography/ultraviolet/evaporative light scattering detection coupled to time-of-flight mass spectrometry (UHPLC/UV/ELSD/TOFMS). Unless otherwise noted, all tested compounds were found to be >95% pure by this method.

UHPLC/MS Analysis. The UHPLC was performed on a Waters ACQUITY UHPLC system (Waters, Milford, MA), which was equipped with a binary solvent delivery manager, column manager, and sample manager coupled to ELSD and UV detectors (Waters, Milford, MA). Detection was performed on a Waters LCT premier XE mass spectrometer (Waters, Milford, MA). The instrument was fitted with an Acquity BEH (bridged ethane hybrid) C18 column (30 mm \times 2.1 mm, 1.7 μ m particle size, Waters, Milford, MA) operated at 60 °C.

Benzyl (2S,4R)-4-Cyano-4-[(3-fluorophenyl)amino]-2-methylpiperidine-1-carboxylate. To a solution of benzyl (2S)-2-methyl-4-oxopiperidine-1-carboxylate^{22,23} (20.0 g, 80.9 mmol) in acetic acid (162 mL) were added 3-fluoroaniline (18.0 g, 162 mmol) and zinc cyanide (23.7 g, 202 mmol). The mixture was allowed to stir overnight at room temperature. The mixture was cooled to 0 °C and quenched with NH_4OH until the mixture was basic. The mixture was filtered to provide a yellow solid, which was combined with further extractions with CH_2Cl_2 , dried with Na_2SO_4 , and concentrated. The material was purified using silica gel chromatography to afford the title compound (29.7 g, 72%). MS (LCMS) m/z 368.1 ($M + 1$). The diastereomeric mixture of benzyl (2S)-4-cyano-4-[(3-fluorophenyl)amino]-2-methylpiperidine-1-carboxylates was subjected to supercritical fluid chromatography to separate the diastereomeric products (column, Chiralcel OJ-H; eluent, 80:20 $CO_2/MeOH$). The (2S,4S) isomer eluted first, followed by the title product (17 g, 47%). MS (LCMS) m/z 368.1 ($M + 1$). ¹H NMR (400 MHz, $CDCl_3$) δ 1.49 (d, $J = 7.2$ Hz, 3H), 1.70 (ddd, $J = 13.1, 13.2, 4.4$ Hz, 1H), 1.89 (dd, $J = 13.9, 6.5$ Hz, 1H), 2.42–2.49 (m, 2H), 3.35 (ddd, $J = 14.6, 13.0, 2.4$ Hz, 1H), 3.74 (s, 1H), 4.27 (m, 1H), 4.63 (m, 1H), 5.14 (d, half of AB quartet, $J = 12.3$ Hz, 1H), 5.18 (d, half of AB quartet, $J = 12.3$ Hz, 1H), 6.60–6.68 (m, 3H), 7.21 (m, 1H), 7.32–7.41 (m, 5H); ¹³C NMR (100 MHz, $CDCl_3$) observed peaks, δ 17.4, 35.9, 36.8, 38.8, 40.3, 46.0, 46.8, 48.5, 50.5, 67.7, 104.8, 107.9, 113.4, 121.4, 128.2, 128.8, 130.7, 136.6, 144.8, 162.5, 164.9. HRMS calcd for $C_{21}H_{23}N_3O_2F$ ($M + 1$) 368.1768, found 368.1766.

Benzyl (2S,4R)-4-(Aminomethyl)-4-[(3-fluorophenyl)amino]-2-methylpiperidine-1-carboxylate (6). To a solution of benzyl (2S,4R)-4-cyano-4-[(3-fluorophenyl)amino]-2-methylpiperidine-1-carboxylate (8.0 g, 21.8 mmol) in a 1 M solution of NH_3 in MeOH (109 mL, 218 mmol) was added Raney nickel in water (1.87 g, 21.8 mol). The mixture was hydrogenated (50 psi) for 12 h, filtered through Celite, and concentrated. Purification by silica gel chromatography (gradient 1–4% MeOH in CH_2Cl_2) provided title compound 6 (7.8 g, 77%). MS (LCMS) m/z 372.1 ($M + 1$). ¹H NMR (400 MHz, $CDCl_3$) δ 1.17 (d, $J = 6.5$ Hz, 3H), 1.56 (dd, $J = 14.4, 8.3$ Hz, 1H), 1.70 (m, 1H), 1.85 (ddd, $J = 13.9, 11.3, 6.2$ Hz, 1H), 2.04 (dd, $J = 14.4, 6.3$ Hz, 1H), 2.87 (d, half of AB quartet, $J = 14$ Hz, 1H), 2.91 (d, half of AB quartet, $J = 14$ Hz, 1H), 3.05 (ddd, $J = 13.9, 11.5, 4.7$ Hz, 1H), 3.93 (ddd, $J = 14.0, 6.0, 2.8$ Hz, 1H), 4.12 (m, 1H), 5.08 (s, 2H), 6.31–6.40 (m, 3H), 6.99 (m, 1H), 7.23–7.31 (m, 5H); ¹³C NMR (100 MHz, $CDCl_3$) observed peaks, δ 19.9, 36.6, 37.6, 46.0, 46.1, 55.6, 56.6, 67.2, 103.1, 105.3, 112.1, 127.9, 128.0, 128.2, 128.7, 130.6, 137.0, 147.5, 155.5, 155.7, 162.7. HRMS calcd for $C_{21}H_{27}N_3O_2F$ ($M + 1$) 372.2081, found 372.2094.

Benzyl (5R,7S)-1-(3-Fluorophenyl)-7-methyl-2-thia-1,3,8-triazaspiro[4.5]decane-8-carboxylate 2,2-Dioxide (9). The triflate salt of mono-*N*-methyl-*N,N'*-sulfuryldiimidazole²⁵ (compound 7, 2.45 g, 6.7 mmol) was dissolved in acetonitrile (20 mL). To this stirred solution was added a solution of 6 (2.0 g, 5.4 mmol) in acetonitrile (10 mL) dropwise via an addition funnel. The solution was stirred at room

temperature for 18 h. The mixture was concentrated under reduced pressure and purified via silica gel chromatography (gradient, 0–35% ethyl acetate in heptane) to provide the product as a white solid (1.0 g, 43%). MS (LCMS) m/z 434.4 ($M + 1$). $^1\text{H NMR}$ (400 MHz, CDCl_3) δ 1.16 (d, $J = 7.2$ Hz, 3H), 1.58 (m, 1H), 1.66–1.75 (m, 2H), 2.02 (br d, $J = 12$ Hz, 1H), 2.94 (m, 1H), 3.60 (dd, $J = 11.6, 9.2$ Hz, 1H), 3.72 (dd, $J = 12.0, 6.9$ Hz, 1H), 4.08 (v br s, 1H), 4.50 (v br s, 1H), 5.05 (d, half of AB quartet, $J = 12.5$ Hz, 1H), 5.09 (d, half of AB quartet, $J = 12.8$ Hz, 1H), 5.56 (dd, $J = 8.7, 7.2$ Hz, 1H), 7.07–7.18 (m, 3H), 7.29–7.37 (m, 5H), 7.39 (ddd, $J = 8.2, 8.2, 6.5$ Hz, 1H); $^{13}\text{C NMR}$ (100 MHz, CDCl_3) observed peaks, δ 32.7, 36.1, 38.8, 46.3, 51.2, 66.1, 67.6, 117.0, 117.2, 120.1, 120.3, 128.0, 128.1, 128.4, 128.8, 130.8, 133.7, 136.5, 161.7, 164.2. HRMS calcd for $\text{C}_{21}\text{H}_{24}\text{N}_3\text{O}_4\text{FS}$ ($M + 1$) 434.1544, found 434.1542.

(5R,7S)-8-Benzyl-1-(3-fluorophenyl)-7-methyl-2-thia-1,3,8-triazaspiro[4.5]decane 2,2-Dioxide (11a). To a solution of **9** (90 mg, 0.2 mmol) in MeOH (2 mL) in a Parr bottle was added palladium hydroxide (15 mg, 0.1 mmol). The mixture was hydrogenated on a Parr shaker at 50 psi overnight. The mixture was filtered and then concentrated to afford (5R,7S)-1-(3-fluorophenyl)-7-methyl-2-thia-1,3,8-triazaspiro[4.5]decane 2,2-dioxide (60 mg, 96%) as a colorless oil. MS (LCMS) m/z 299.37 ($M + 1$). $^1\text{H NMR}$ (400 MHz, CDCl_3) δ 0.98 (d, $J = 6.3$ Hz, 3H), 1.37 (dd, $J = 14.3, 10.9$ Hz, 1H), 1.69 (ddd, $J = 14.4, 12.2, 4.7$ Hz, 1H), 2.17–2.22 (m, 2H), 2.46 (ddd, $J = 12.5, 12.5, 2.8$ Hz, 1H), 2.56 (m, 1H), 2.80 (ddd, $J = 12.8, 4.6, 3.5$ Hz, 1H), 3.29 (d, half of AB quartet, $J = 11.9$ Hz, 1H), 3.34 (d, half of AB quartet, $J = 12.0$ Hz, 1H), 7.08–7.14 (m, 2H), 7.19 (ddd, $J = 8.0, 2.0, 1.0$ Hz, 1H), 7.36 (dddd, $J = 8.0, 8.0, 6.4, 0.8$ Hz, 1H).

To a solution of (5R,7S)-1-(3-fluorophenyl)-7-methyl-2-thia-1,3,8-triazaspiro[4.5]decane 2,2-dioxide (28 mg, 0.095 mmol) and benzaldehyde (19.8 mg, 0.187 mmol) in dichloroethane (0.94 mL) was added acetic acid (5.6 mg, 0.095 mmol). The mixture was allowed to stir at room temperature for 5 h, then was charged with sodium triacetoxyborohydride (40 mg, 0.18 mmol) and stirred overnight. The reaction was quenched with aqueous NaHCO_3 solution, extracted with CH_2Cl_2 , dried over Na_2SO_4 , filtered, and concentrated. Purification by silica gel chromatography using a 20–100% gradient of ethyl acetate/heptane provided the title compound **11a** (34 mg, 86%). MS (LCMS) m/z 390.1 ($M + 1$). $^1\text{H NMR}$ (400 MHz, CDCl_3) δ 7.36 (m, 1H), 7.07–7.31 (m, 8H), 4.96 (br s, 1H), 3.63 (d, $J = 13.7$ Hz, 1H), 3.42–3.58 (m, 2H), 3.31 (d, $J = 13.3$ Hz, 1H), 2.64–2.76 (m, 1H), 2.43–2.58 (m, 1H), 2.19–2.32 (m, 1H), 1.92–2.07 (m, 2H), 1.75–1.88 (m, 1H), 1.61 (dd, $J = 5.8, 13.7$ Hz, 1H), 1.04 (d, $J = 6.2$ Hz, 3H). HRMS calcd for $\text{C}_{20}\text{H}_{25}\text{N}_3\text{O}_2\text{FS}$ ($M + 1$) 390.1632, found 390.1646.

(5R,7S)-1-(3-Fluorophenyl)-8-(3-methoxybenzyl)-7-methyl-2-thia-1,3,8-triazaspiro[4.5]decane 2,2-Dioxide (11b). To a solution of (5R,7S)-1-(3-fluorophenyl)-7-methyl-2-thia-1,3,8-triazaspiro[4.5]decane 2,2-dioxide (16 mg, 0.053 mmol) and 3-methoxybenzaldehyde (14.4 mg, 0.106 mmol) in dichloroethane (0.53 mL) was added acetic acid (3.2 mg, 0.053 mmol). The mixture was allowed to stir at room temperature for 5 h, then was charged with sodium triacetoxyborohydride (22.5 mg, 0.106 mmol) and stirred overnight. The reaction was quenched with aqueous NaHCO_3 solution, extracted with CH_2Cl_2 , dried over Na_2SO_4 , filtered, and concentrated. Purification by silica gel chromatography using a 20–100% gradient of ethyl acetate/heptane provided the first eluent (6 mg, 25%) of the title compound **11b**. MS (LCMS) m/z 420.0 ($M + 1$). $^1\text{H NMR}$ (400 MHz, CDCl_3) δ 7.32–7.45 (m, 1H), 7.06–7.24 (m, 4H), 6.71–6.81 (m, 3H), 4.61–4.74 (m, 1H), 3.77 (s, 3H), 3.44–3.65 (m, 3H), 3.28 (d, $J = 13.3$ Hz, 1H), 2.64–2.76 (m, 1H), 2.47–2.57 (m, 1H), 2.19–2.32 (m, 1H), 1.93–2.05 (m, 2H), 1.77–1.87 (m, 1H), 1.55–1.65 (m, 1H), 1.05 (d, $J = 6.6$ Hz, 3H). HRMS calcd for $\text{C}_{22}\text{H}_{26}\text{N}_3\text{O}_3\text{FS}$ ($M + 1$) 420.1743, found 420.1751.

(5R,7S)-8-(3-Ethoxybenzyl)-1-(3-fluorophenyl)-7-methyl-2-thia-1,3,8-triazaspiro[4.5]decane 2,2-Dioxide (11c). To a solution of (5R,7S)-1-(3-fluorophenyl)-7-methyl-2-thia-1,3,8-triazaspiro[4.5]decane 2,2-dioxide (12 mg, 0.040 mmol) and 3-ethoxybenzaldehyde (12 mg, 0.08 mmol) in dichloroethane (0.4 mL) was added triethylamine (8.1 mg, 0.08 mmol). The mixture was allowed to stir at room temperature for 30 min, then was charged with

sodium triacetoxyborohydride (10.2 mg, 0.048 mmol) and stirred overnight. The reaction was quenched with aqueous NaHCO_3 solution, extracted with CH_2Cl_2 , dried over Na_2SO_4 , filtered, and concentrated. Purification by silica gel chromatography using a 0–3% gradient of methanol/dichloromethane provided the first eluent (6.6 mg, 38%) of the title compound **11c**. MS (LCMS) m/z 434 ($M + 1$). $^1\text{H NMR}$ (400 MHz, CDCl_3) δ 7.34 (td, $J = 8.1, 6.4$ Hz, 1H), 7.02–7.16 (m, 4H), 6.67–6.80 (m, 3H), 4.63 (br s, 1H), 3.96 (q, $J = 6.9$ Hz, 2H), 3.59 (d, $J = 13.5$ Hz, 1H), 3.48 (q, $J = 12.2$ Hz, 2H), 3.25 (d, $J = 13.5$ Hz, 1H), 2.61–2.74 (m, 1H), 2.49 (td, $J = 8.4, 4.2$ Hz, 1H), 2.17–2.30 (m, 1H), 1.90–2.01 (m, 2H), 1.72–1.86 (m, 1H), 1.58 (dd, $J = 13.6, 6.4$ Hz, 1H), 1.36 (t, $J = 6.9$ Hz, 3H), 1.02 (d, $J = 6.6$ Hz, 3H). HRMS calcd for $\text{C}_{22}\text{H}_{29}\text{N}_3\text{O}_3\text{FS}$ ($M + 1$) 434.1908, found 434.1911.

(5R,7S)-1-(3-Fluorophenyl)-8-(3-isopropoxybenzyl)-7-methyl-2-thia-1,3,8-triazaspiro[4.5]decane 2,2-Dioxide (11d). To a solution of (5R,7S)-1-(3-fluorophenyl)-7-methyl-2-thia-1,3,8-triazaspiro[4.5]decane 2,2-dioxide (12 mg, 0.040 mmol) and 3-isopropoxybenzaldehyde (12 mg, 0.08 mmol) in dichloroethane (0.4 mL) was added triethylamine (8.1 mg, 0.08 mmol). The mixture was allowed to stir at room temperature for 30 min, then was charged with sodium triacetoxyborohydride (10.2 mg, 0.048 mmol) and stirred overnight. The reaction was quenched with aqueous NaHCO_3 solution, extracted with CH_2Cl_2 , dried over Na_2SO_4 , filtered, and concentrated. Purification by silica gel chromatography using a 0–3% gradient of methanol/dichloromethane provided the first eluent (11.6 mg, 65.2%) of the title compound **11d**. MS (LCMS) m/z 448.6 ($M + 1$). $^1\text{H NMR}$ (400 MHz, CDCl_3) δ 7.30 (d, $J = 7.4$ Hz, 1H), 7.03–7.18 (m, 4H), 6.67–6.78 (m, 3H), 5.50–5.87 (m, 1H), 4.40–4.53 (m, 1H), 3.58 (d, $J = 13.5$ Hz, 1H), 3.45–3.52 (m, 1H), 3.37–3.44 (m, 1H), 3.30 (d, $J = 13.5$ Hz, 1H), 2.64–2.76 (m, 1H), 2.44–2.55 (m, 1H), 2.18–2.27 (m, 1H), 1.87–2.00 (m, $J = 4.5$ Hz, 2H), 1.77–1.87 (m, 1H), 1.55–1.66 (m, 1H), 1.26 (d, $J = 6.0$ Hz, 6H), 1.01 (d, $J = 6.8$ Hz, 3H). HRMS calcd for $\text{C}_{23}\text{H}_{30}\text{N}_3\text{O}_3\text{FS}$ ($M + 1$) 448.2081, found 448.2064.

(5R,7S)-1-(3-Fluorophenyl)-7-methyl-8-(3-propoxybenzyl)-2-thia-1,3,8-triazaspiro[4.5]decane 2,2-Dioxide (11e). To a solution of (5R,7S)-1-(3-fluorophenyl)-7-methyl-2-thia-1,3,8-triazaspiro[4.5]decane 2,2-dioxide (12 mg, 0.040 mmol) and 3-propoxybenzaldehyde (12 mg, 0.08 mmol) in dichloroethane (0.4 mL) was added triethylamine (8.1 mg, 0.08 mmol). The mixture was allowed to stir at room temperature for 30 min, then was charged with sodium triacetoxyborohydride (10.2 mg, 0.048 mmol) and stirred overnight. The reaction was quenched with aqueous NaHCO_3 solution, extracted with CH_2Cl_2 , dried over Na_2SO_4 , filtered, and concentrated. Purification by silica gel chromatography using a 0–3% gradient of methanol/dichloromethane provided the first eluent (8.5 mg, 48%) of the title compound **11e**. MS (LCMS) m/z 448.5 ($M + 1$). $^1\text{H NMR}$ (400 MHz, CDCl_3) δ 7.31–7.44 (m, 1H), 7.05–7.20 (m, 4H), 6.70–6.81 (m, 3H), 4.80 (br s, 1H), 3.87 (t, $J = 6.6$ Hz, 2H), 3.60 (d, $J = 13.7$ Hz, 1H), 3.43–3.59 (m, 2H), 3.27 (d, $J = 13.3$ Hz, 1H), 2.63–2.77 (m, 1H), 2.51 (dt, $J = 3.9, 8.4$ Hz, 1H), 2.19–2.32 (m, 1H), 1.92–2.04 (m, 2H), 1.72–1.87 (m, 3H), 1.60 (dd, $J = 5.8, 13.7$ Hz, 1H), 0.96–1.08 (m, 6H). HRMS calcd for $\text{C}_{23}\text{H}_{30}\text{N}_3\text{O}_3\text{FS}$ ($M + 1$) 448.2060, found 448.2064.

(5R,7S)-1-(3-Fluorophenyl)-8-(3-isobutoxybenzyl)-7-methyl-2-thia-1,3,8-triazaspiro[4.5]decane 2,2-Dioxide (11f). To a solution of (5R,7S)-1-(3-fluorophenyl)-7-methyl-2-thia-1,3,8-triazaspiro[4.5]decane 2,2-dioxide (12 mg, 0.040 mmol) and 3-isobutoxybenzaldehyde (12 mg, 0.08 mmol) in dichloroethane (0.4 mL) was added triethylamine (8.1 mg, 0.08 mmol). The mixture was allowed to stir at room temperature for 30 min, then was charged with sodium triacetoxyborohydride (10.2 mg, 0.048 mmol) and stirred overnight. The reaction was quenched with aqueous NaHCO_3 solution, extracted with CH_2Cl_2 , dried over Na_2SO_4 , filtered, and concentrated. Purification by silica gel chromatography using a 0–3% gradient of methanol/dichloromethane provided the first eluent (8.5 mg, 46%) of the title compound **11f**. MS (LCMS) m/z 462.3 ($M + 1$). $^1\text{H NMR}$ (400 MHz, CDCl_3) δ 7.27–7.40 (m, 1H), 7.04–7.17 (m, 4H), 6.68–6.78 (m, 3H), 4.73 (br s, 1H), 3.61–3.67 (m, 2H), 3.59 (d,

$J = 13.5$ Hz, 1H), 3.48 (q, $J = 12.1$ Hz, 2H), 3.25 (d, $J = 13.5$ Hz, 1H), 2.61–2.73 (m, 1H), 2.43–2.55 (m, 1H), 2.17–2.30 (m, 1H), 1.90–2.08 (m, 3H), 1.73–1.86 (m, 1H), 1.59 (dd, $J = 13.7$, 6.0 Hz, 1H), 1.02 (d, $J = 6.6$ Hz, 3H), 0.98 (dd, $J = 6.6$, 2.0 Hz, 6H). HRMS calcd for $C_{24}H_{33}N_3O_3FS$ ($M + 1$) 462.2221, found 448.2212.

(5R,7S)-8-[3-(Cyclopentyl-oxo)benzyl]-1-(3-fluorophenyl)-7-methyl-2-thia-1,3,8-triazaspiro[4.5]decane 2,2-Dioxide (11g). To a solution of (5R,7S)-1-(3-fluorophenyl)-7-methyl-2-thia-1,3,8-triazaspiro[4.5]decane 2,2-dioxide (12 mg, 0.040 mmol) and 3-cyclopentyl-oxo-benzaldehyde (15.2 mg, 0.08 mmol) in dichloroethane (0.4 mL) was added triethylamine (8.1 mg, 0.08 mmol). The mixture was allowed to stir at room temperature for 30 min, then was charged with sodium triacetoxyborohydride (10.2 mg, 0.048 mmol) and stirred overnight. The reaction was quenched with aqueous $NaHCO_3$ solution, extracted with CH_2Cl_2 , dried over Na_2SO_4 , filtered, and concentrated. Purification by silica gel chromatography using a 0–3% gradient of methanol/dichloromethane provided the first eluent (6.2 mg, 30%) of the title compound **11g**. MS (LCMS) m/z 474.0 ($M + 1$). 1H NMR (400 MHz, $CDCl_3$) δ 7.30–7.43 (m, 1H), 7.03–7.18 (m, 4H), 6.65–6.78 (m, 3H), 4.59–4.74 (m, 2H), 3.58 (d, $J = 13.5$ Hz, 1H), 3.43–3.55 (m, 2H), 3.25 (d, $J = 13.5$ Hz, 1H), 2.64–2.77 (m, 1H), 2.50 (ddd, $J = 12.4$, 8.6, 3.5 Hz, 1H), 2.16–2.32 (m, 1H), 1.90–2.01 (m, 2H), 1.69–1.89 (m, 7H), 1.50–1.64 (m, 3H), 1.02 (d, $J = 6.8$ Hz, 3H). HRMS calcd for $C_{25}H_{32}N_3O_3FS$ ($M + 1$) 474.2221, found 474.2211.

(5R,7S)-8-[(2'-Chlorobiphenyl-3-yl)methyl]-1-(3-fluorophenyl)-7-methyl-2-thia-1,3,8-triazaspiro[4.5]decane 2,2-Dioxide (11h). To a solution of (5R,7S)-1-(3-fluorophenyl)-7-methyl-2-thia-1,3,8-triazaspiro[4.5]decane 2,2-dioxide (40 mg, 0.13 mmol) and 3-iodobenzaldehyde (62.2 mg, 0.268 mmol) in dichloroethane (1.34 mL) was added triethylamine (27.1 mg, 0.268 mmol). The mixture was allowed to stir at room temperature for 30 min, then was charged with sodium triacetoxyborohydride (34.1 mg, 0.161 mmol) and stirred overnight. The reaction was quenched with aqueous $NaHCO_3$ solution, extracted with CH_2Cl_2 , dried over Na_2SO_4 , filtered, and concentrated. Purification by silica gel chromatography using a 0–3% gradient of methanol/dichloromethane provided 43.6 mg (63%) of (5R,7S)-8-[3-iodobenzyl]-1-(3-fluorophenyl)-7-methyl-2-thia-1,3,8-triazaspiro[4.5]decane 2,2-dioxide. MS (LCMS) m/z 516.1 ($M + 1$). 1H NMR (400 MHz, $CDCl_3$) δ 7.48–7.58 (m, 2H), 7.29–7.42 (m, 1H), 7.05–7.18 (m, 4H), 6.91–7.01 (m, 1H), 4.97–5.14 (m, 1H), 3.38–3.61 (m, 3H), 3.20 (d, $J = 13.7$ Hz, 1H), 2.56–2.69 (m, 1H), 2.45 (ddd, $J = 3.4$, 8.2, 12.2 Hz, 1H), 2.12–2.24 (m, 1H), 1.87–2.05 (m, 2H), 1.73–1.85 (m, 1H), 1.58 (dd, $J = 6.2$, 13.7 Hz, 1H), 1.00 (d, $J = 6.6$ Hz, 3H).

To a solution of (5R,7S)-8-[3-iodobenzyl]-1-(3-fluorophenyl)-7-methyl-2-thia-1,3,8-triazaspiro[4.5]decane 2,2-dioxide (40 mg, 0.078 mmol) were added Na_2CO_3 (41.3 mg, 0.39 mmol), 2-chlorobiphenylboronic acid (24.4 mg, 0.156 mmol), ethanol (0.78 mL), and water (0.2 mL). Dry nitrogen was bubbled through the reaction mixture for 5 min in order to degas the solvent. Tetrakis(triphenylphosphine)palladium(0) (9.4 mg, 10 mol %) was then added. The vial was sealed, and the mixture was heated to 50 °C for 18 h. The reaction was quenched with aqueous $NaHCO_3$ solution, extracted with CH_2Cl_2 , dried over Na_2SO_4 , filtered, and concentrated. Purification by silica gel chromatography using a 0–4% gradient of methanol/dichloromethane provided the first eluent (8.4 mg, 22%) of the title compound **11h**. MS (LCMS) m/z 500.2 ($M + 1$). 1H NMR (400 MHz, $CDCl_3$) δ 7.40–7.46 (m, 1H), 7.24–7.37 (m, 7H), 7.06–7.20 (m, 4H), 4.67 (t, $J = 8.0$ Hz, 1H), 3.68 (d, $J = 13.7$ Hz, 1H), 3.42–3.59 (m, 2H), 3.32 (d, $J = 13.5$ Hz, 1H), 2.66–2.75 (m, 1H), 2.54 (ddd, $J = 12.4$, 8.3, 3.5 Hz, 1H), 2.24–2.32 (m, 1H), 1.93–2.01 (m, 2H), 1.76–1.86 (m, 1H), 1.57–1.63 (m, 1H), 1.04 (d, $J = 6.6$ Hz, 3H). HRMS calcd for $C_{26}H_{27}N_3O_2FSCI$ ($M + 1$) 500.1569, found 500.1558.

(5R,7S)-1-(3-Fluorophenyl)-8-(3-isopropoxybenzyl)-3,7-dimethyl-2-thia-1,3,8-triazaspiro[4.5]decane 2,2-Dioxide (12a). (5R,7S)-1-(3-Fluorophenyl)-8-(3-isopropoxybenzyl)-7-methyl-2-thia-1,3,8-triazaspiro[4.5]decane 2,2-dioxide **11d** (20 mg, 0.045 mmol) was added to a slurry of NaH (3.6 mg, 0.09 mmol) in DMF (0.6 mL) at 0 °C. The mixture was stirred at 0 °C for 2 h. Then methyl iodide (8.7

mg, 0.061 mmol) in DMF (0.2 mL) was added. The mixture was allowed to gradually warm to room temperature and stirred overnight. The mixture was diluted with water and extracted with ethyl acetate (3 \times 10 mL). The combined organics were dried over Na_2SO_4 , concentrated, and purified by silica gel chromatography to yield the title compound **12a** (15 mg, 67%). 1H NMR (400 MHz, CD_3OD) δ 7.45 (dt, $J = 6.4$, 8.1 Hz, 1H), 7.12–7.29 (m, 4H), 6.72–6.87 (m, 3H), 4.56 (spt, $J = 6.0$ Hz, 1H), 3.69 (d, $J = 13.3$ Hz, 1H), 3.57 (d, $J = 9.4$ Hz, 1H), 3.49 (d, $J = 13.7$ Hz, 1H), 3.29–3.34 (m, 1H), 2.81 (s, 3H), 2.65–2.76 (m, 2H), 2.32–2.43 (m, 1H), 2.06–2.21 (m, 2H), 1.92–2.02 (m, 1H), 1.73 (dd, $J = 7.0$, 14.0 Hz, 1H), 1.31 (dd, $J = 1.2$, 5.8 Hz, 6H), 1.16 (d, $J = 6.6$ Hz, 3H); ^{13}C NMR (100 MHz, CD_3OD) δ 163.8, 161.3, 157.9, 135.3, 130.2, 129.0, 121.3, 120.1, 116.6, 114.6, 69.4, 61.3, 60.3, 56.9, 51.3, 44.5, 41.5, 33.6, 31.8, 21.0, 15.0; LCMS m/z 462.3 ($M + 1$); HRMS calcd for $C_{24}H_{32}N_3O_3FS$ ($M + 1$) 462.2221, found 462.2224.

(5R,7S)-3-Ethyl-1-(3-fluorophenyl)-8-(3-isopropoxybenzyl)-7-methyl-2-thia-1,3,8-triazaspiro[4.5]decane 2,2-Dioxide (12b). (5R,7S)-1-(3-Fluorophenyl)-8-(3-isopropoxybenzyl)-7-methyl-2-thia-1,3,8-triazaspiro[4.5]decane 2,2-dioxide (25 mg, 0.061 mmol) was added to a slurry of NaH (4.9 mg, 0.09 mmol) in DMF (0.61 mL) at 0 °C. The mixture was stirred at 0 °C for 2 h. Then iodoethane (8.7 mg, 0.061 mmol) in DMF (0.2 mL) was added. The mixture was allowed to gradually warm to room temperature and stirred overnight. The mixture was diluted with water and extracted with ethyl acetate (3 \times 10 mL). The combined organics were dried over Na_2SO_4 and concentrated to yield the title compound **12b** (20 mg, 93%). LCMS m/z 476.3 ($M + 1$). 1H NMR (400 MHz, $CDCl_3$) δ 1.03 (d, $J = 6.6$ Hz, 3H), 1.28 (d, $J = 6.1$ Hz, 6H), 1.30 (t, $J = 7.2$ Hz, 3H), 1.62 (ddd, $J = 13.6$, 5.5, 1.4 Hz, 1H), 1.85–1.97 (m, 2H), 2.03 (dd, $J = 13.4$, 5.0 Hz, 1H), 2.23–2.34 (m, 1H), 2.48–2.57 (m, 1H), 2.73–2.80 (m, 1H), 3.09 (dd, $J = 12.9$, 7.2 Hz, 1H), 3.18–3.31 (m, 3H), 3.42 (d, $J = 9.2$ Hz, 1H), 3.56 (d, $J = 13.5$ Hz, 1H), 4.43–4.53 (m, 1H), 6.68–6.76 (m, 3H), 7.06–7.21 (m, 4H), 7.30–7.41 (m, 1H), 476.3 ($M + 1$). HRMS calcd for $C_{25}H_{34}N_3O_3FS$ ($M + 1$) 476.2388, found 476.2377.

(5R,7S)-1-(3-Fluorophenyl)-8-(3-isopropoxybenzyl)-3-isopropyl-7-methyl-2-thia-1,3,8-triazaspiro[4.5]decane 2,2-Dioxide (12c). (5R,7S)-1-(3-Fluorophenyl)-8-(3-isopropoxybenzyl)-7-methyl-2-thia-1,3,8-triazaspiro[4.5]decane 2,2-dioxide (25 mg, 0.045 mmol) was added to a slurry of NaH (4.9 mg, 0.1 mmol) in DMF (0.1 M, 0.45 mL) at 0 °C. The mixture was stirred at 0 °C for 2 h. Then 2-iodopropane (8.7 mg, 0.045 mmol) in DMF (0.2 mL) was added. The mixture was allowed to gradually warm to room temperature and stirred overnight. The mixture was diluted with water and extracted with ethyl acetate (3 \times 10 mL). The combined organics were dried over Na_2SO_4 , concentrated, and purified by silica gel chromatography to yield the title compound **12c** (5 mg, 20%). MS (LCMS) m/z 490.3 ($M + 1$). 1H NMR (400 MHz, $CDCl_3$) δ 1.03 (d, $J = 6.6$ Hz, 3H), 1.28 (d, $J = 6.0$ Hz, 6H), 1.31 (d, $J = 6.6$ Hz, 6H), 1.55 (s, 1H), 1.62 (dd, $J = 12.5$, 6.0 Hz, 1H), 1.82–1.89 (m, 1H), 1.94 (dd, $J = 8.2$, 4.3 Hz, 1H), 2.05 (dd, $J = 14.1$, 4.3 Hz, 1H), 2.22–2.32 (m, 1H), 2.45–2.56 (m, 1H), 2.70–2.76 (m, 1H), 3.23–3.30 (m, 2H), 3.34–3.41 (m, 1H), 3.58 (d, $J = 13.5$ Hz, 1H), 3.75–3.84 (m, 1H), 4.44–4.52 (m, 1H), 6.72 (d, $J = 2.0$ Hz, 1H), 6.73 (s, 2H), 7.09–7.19 (m, 4H), 7.30–7.39 (m, 1H). HRMS calcd for $C_{26}H_{36}N_3O_3FS$ ($M + 1$) 490.2541, found 490.2534.

(5R,7S)-1-(3-Fluorophenyl)-3,7-dimethyl-2-thia-1,3,8-triazaspiro[4.5]decane 2,2-Dioxide (13). A solution of **9** (611 mg, 1.41 mmol) in DMF (7 mL) was added to a slurry of NaH (110 mg, 2.8 mmol) in DMF (7 mL) at 0 °C. The mixture was stirred at 0 °C for 30 min. Methyl iodide (202 mg, 1.41 mmol) was then added. The mixture was allowed to gradually warm to room temperature and stirred overnight. The mixture was diluted with water and extracted with ethyl acetate (3 \times 10 mL). The combined organics were dried over Na_2SO_4 , concentrated, and purified by silica gel chromatography to yield benzyl (5R,7S)-1-(3-fluorophenyl)-3,7-dimethyl-2-thia-1,3,8-triazaspiro[4.5]decane-8-carboxylate 2,2-dioxide (560 mg, 89%). MS (LCMS) m/z 448.0 ($M + 1$). 1H NMR (400 MHz, $CDCl_3$) δ 1.21 (d, $J = 7.2$ Hz, 3H), 1.66 (m, 1H), 1.73–1.82 (m, 2H), 2.10 (br d, $J = 13$ Hz, 1H), 2.85 (s, 3H), 3.03 (v br dd, $J = 14$, 14 Hz, 1H), 3.38 (br d, J

= 9.3 Hz, 1H), 3.62 (d, $J = 9.3$ Hz, 1H), 4.16 (v br s, 1H), 4.53 (v br s, 1H), 5.06 (br s, 2H), 7.10 (ddd, $J = 9.3, 2.2, 2.2$ Hz, 1H), 7.15–7.21 (m, 2H), 7.28–7.37 (m, 5H), 7.41 (ddd, $J = 8.2, 8.2, 6.4$ Hz, 1H). HRMS calcd for $C_{22}H_{26}N_3O_4FS$ ($M + 1$) 448.1700, found 448.1680.

To a solution of benzyl (SR,7S)-1-(3-fluorophenyl)-3,7-methyl-2-thia-1,3,8-triazaspiro[4.5]decane-8-carboxylate 2,2-dioxide (549 mg, 1.23 mmol) in MeOH (10 mL) was added palladium hydroxide (150 mg, 0.21 mmol). The mixture was hydrogenated at 50 psi for 3 h. The mixture was filtered and then concentrated to afford the title compound **13** as a white foam (405 mg, quantitative). MS (LCMS) m/z 314.0 ($M + 1$). 1H NMR (400 MHz, $CDCl_3$) δ 1.00 (d, $J = 6.4$ Hz, 3H), 1.41 (dd, $J = 14.0, 10.0$ Hz, 1H), 1.76 (ddd, $J = 14.1, 11.2, 4.6$ Hz, 1H), 2.22–2.31 (m, 2H), 2.55 (ddd, $J = 12.8, 11.3, 3.0$ Hz, 1H), 2.66 (m, 1H), 2.80–2.86 (m, 1H), 2.83 (s, 3H), 3.21 (d, half of AB quartet, $J = 9.3$ Hz, 1H), 3.28 (d, half of AB quartet, $J = 9.3$ Hz, 1H), 7.13–7.22 (m, 2H), 7.27 (ddd, $J = 8.0, 1.9, 1.1$ Hz, 1H), 7.40 (ddd, $J = 8.1, 8.1, 6.4$ Hz, 1H); ^{13}C NMR (100 MHz, $CDCl_3$) observed peaks, δ 21.5, 33.4, 35.1, 41.0, 43.4, 47.5, 61.0, 62.7, 117.3, 120.7, 129.2, 130.7, 161.6, 164.1. HRMS calcd for $C_{14}H_{20}N_3O_2FS$ ($M + 1$) 314.1333, found 314.1346.

(SR,7S)-1-(3-Fluorophenyl)-8-(3-isopropoxybenzyl)-7-methyl-3-(1,3-oxazol-2-yl)-2-thia-1,3,8-triazaspiro[4.5]decane 2,2-Dioxide (12h). To a dry sealed flask were added **11d** (35.8 mg, 0.080 mmol), 2-iodooxazole (46.5 mg, 0.239 mmol), copper(I) iodide (46.0 mg, 0.239 mmol), potassium carbonate (33.0 mg, 0.239 mmol), N,N' -dimethylethane-1,2-diamine (34 μ L, 0.319 mmol), and dioxane (2 mL). The suspension was heated overnight at 105 °C, then cooled to room temperature and filtered through Celite. The filter pad was washed with ethyl acetate (20 mL), and the combined filtrates were washed with saturated aqueous sodium bicarbonate solution (15 mL), dried over sodium sulfate, filtered, and concentrated in vacuo. The residue was purified by chromatography on silica gel (gradient, 0–100% ethyl acetate in heptane) to provide **12h** as a white solid (12.5 mg, 30%). 1H NMR (500 MHz, $CDCl_3$) δ 1.11 (d, $J = 6.7$ Hz, 3H), 1.32 (d, $J = 6.1$ Hz, 6H), 1.71 (br dd, $J = 13.6, 6.0$ Hz, 1H), 2.01 (m, 1H), 2.07–2.14 (m, 2H), 2.37 (ddd, $J = 12.8, 6.7, 3.7$ Hz, 1H), 2.62 (ddd, $J = 12.6, 8.4, 3.5$ Hz, 1H), 2.82 (m, 1H), 3.34 (d, half of AB quartet, $J = 13.5$ Hz, 1H), 3.64 (d, half of AB quartet, $J = 13.5$ Hz, 1H), 4.08 (d, half of AB quartet, $J = 9.9$ Hz, 1H), 4.24 (d, half of AB quartet, $J = 9.8$ Hz, 1H), 4.51 (septet, $J = 6.1$ Hz, 1H), 6.75–6.78 (m, 3H), 7.01 (d, $J = 1.0$ Hz, 1H), 7.15–7.24 (m, 4H), 7.43 (ddd, $J = 8.1, 8.1, 6.2$ Hz, 1H), 7.51 (d, $J = 1.1$ Hz, 1H). ^{13}C NMR ($CDCl_3$) δ 15.87, 22.22, 22.25, 33.64, 41.59, 44.57, 51.33, 57.33, 57.98, 62.85, 69.87, 114.31, 116.52, 117.54, 120.62, 121.01, 127.11, 129.13, 129.38, 130.68, 134.04, 136.81, 140.22, 153.29, 158.11, 161.61. HRMS [$M + H$]⁺ calcd for $C_{26}H_{32}N_4O_4FS$ 515.2122, found 515.2121.

(SR,7S)-1-(3-Fluorophenyl)-8-(3-isopropoxybenzyl)-7-methyl-3-(1,3-thiazol-2-yl)-2-thia-1,3,8-triazaspiro[4.5]decane 2,2-Dioxide (12g). Application of the method used to make **12h** from **11d**, using 2-iodothiazole in place of 2-iodooxazole, afforded **12g** as a white solid (17.6 mg, 41%). 1H NMR (500 MHz $CDCl_3$) δ 7.46 (d, $J = 3.4$ Hz, 1H), 7.43 (td, $J = 8.1, 6.5$ Hz, 1H), 7.14–7.25 (m, 4H), 7.01 (d, $J = 3.4$ Hz, 1H), 6.73–6.79 (m, 3H), 4.51 (spt, $J = 6.0$ Hz, 1H), 4.33 (d, $J = 10.0$ Hz, 1H), 4.13 (d, $J = 10.0$ Hz, 1H), 3.63 (d, $J = 13.7$ Hz, 1H), 3.34 (d, $J = 13.4$ Hz, 1H), 2.79–2.87 (m, 1H), 2.62 (ddd, $J = 12.5, 8.6, 3.3$ Hz, 1H), 2.37 (ddd, $J = 12.5, 6.6, 4.0$ Hz, 1H), 2.04–2.16 (m, 2H), 1.95–2.03 (m, 1H), 1.73 (ddd, $J = 13.7, 5.8, 1.2$ Hz, 1H), 1.31 (d, $J = 6.1$ Hz, 6H), 1.12 (d, $J = 6.8$ Hz, 3H). HRMS [$M + H$]⁺ calcd for $C_{26}H_{32}N_4O_3FS_2$ 531.1894, found 531.1897.

(SR,7S)-1-(3-Fluorophenyl)-8-(3-isopropoxybenzyl)-7-methyl-3-(pyridin-3-yl)-2-thia-1,3,8-triazaspiro[4.5]decane 2,2-Dioxide (12e). Application of the method used to make **12h** from **11d**, using 3-bromopyridine in place of 2-iodooxazole, afforded **12e** as a white solid (10.2 mg, 49%). 1H NMR (500 MHz $CDCl_3$) δ 1.14 (br s, 3H), 1.32 (d, $J = 5.9$ Hz, 3H), 1.71–1.84 (m, 1H), 2.03–2.26 (m, 1H), 2.34–2.41 (m, 1H), 2.57–2.68 (m, 1H), 2.79–2.87 (m, 2H), 3.29–3.39 (m, 1H), 3.62–3.73 (m, 1H), 3.89 (d, half of AB quartet, $J = 8.8$ Hz, 1H), 3.93 (d, half of AB quartet, $J = 8.8$ Hz, 1H), 4.48–4.55 (m, 1H), 6.75–6.81 (m, 3H), 7.14–7.25 (m, 4H), 7.35 (dd, $J = 4.6$ Hz, 8.3 Hz, 1H), 7.39–7.45 (m, 1H), 7.81 (d, $J = 9.5$ Hz, 1H), 8.47

(br s, 1H), 8.55 (br s, 1H). HRMS [$M + H$]⁺ calcd for $C_{28}H_{34}N_4O_3FS$ 525.2330, found 525.2324.

(SR,7S)-1-(3-Fluorophenyl)-8-(3-isopropoxybenzyl)-7-methyl-3-(pyridin-4-yl)-2-thia-1,3,8-triazaspiro[4.5]decane 2,2-Dioxide (12d). To a sealed, dry flask were added **9** (53.3 mg, 0.123 mmol), 4-bromopyridine hydrochloride (71.8 mg, 0.369 mmol), copper(I) iodide (71.0 mg, 0.369 mmol), potassium carbonate (102.0 mg, 0.738 mmol), N,N' -dimethylethane-1,2-diamine (52 μ L, 0.492 mmol), and dioxane (3 mL). The suspension was heated overnight at 105 °C, then cooled to room temperature and filtered through Celite. The filter pad was washed with ethyl acetate (20 mL), and the combined filtrates were washed with saturated aqueous sodium bicarbonate solution (15 mL), dried over sodium sulfate, filtered, and concentrated in vacuo. The residue was purified by chromatography on silica gel (gradient, 0–100% ethyl acetate in heptane) to provide benzyl (SR,7S)-1-(3-fluorophenyl)-7-methyl-3-(pyridin-4-yl)-2-thia-1,3,8-triazaspiro[4.5]decane-8-carboxylate 2,2-dioxide as a white solid (42.8 mg, 68%). MS (ESI) m/z : 511.2 ($M + 1$). 1H NMR (400 MHz, $CDCl_3$) δ 8.03–9.25 (m, 2H), 7.43 (td, $J = 8.2, 6.4$ Hz, 1H), 7.18–7.34 (m, 9H), 7.14 (dt, $J = 9.0, 2.2$ Hz, 1H), 5.04 (s, 2H), 4.51–4.63 (m, 1H), 4.19 (d, $J = 12.5$ Hz, 1H), 4.06 (d, $J = 8.8$ Hz, 1H), 3.94 (d, $J = 8.4$ Hz, 1H), 3.04 (t, $J = 13.3$ Hz, 1H), 2.21 (d, $J = 13.9$ Hz, 1H), 1.70–1.85 (m, 3H), 1.25 (d, $J = 7.2$ Hz, 3H).

To a solution of benzyl (SR,7S)-1-(3-fluorophenyl)-7-methyl-3-(pyridin-4-yl)-2-thia-1,3,8-triazaspiro[4.5]decane-8-carboxylate 2,2-dioxide (42 mg, 0.082 mmol) in MeOH (5 mL) was added 20% palladium hydroxide on carbon (25 mg, 0.036 mmol). The mixture was hydrogenated at 40 psi overnight. The mixture was filtered and concentrated to afford (SR,7S)-1-(3-fluorophenyl)-7-methyl-3-(pyridin-4-yl)-2-thia-1,3,8-triazaspiro[4.5]decane 2,2-dioxide as a colorless oil, which was used in the next reaction without further purification (31 mg, 0.082 mmol). To a suspension of (SR,7S)-1-(3-fluorophenyl)-7-methyl-3-(pyridin-4-yl)-2-thia-1,3,8-triazaspiro[4.5]decane 2,2-dioxide (0.082 mmol) and cesium carbonate (80.2 mg, 0.246 mmol) in DMF (1.5 mL) was added 1-(bromomethyl)-3-isopropoxybenzene (37.6 mg, 0.164 mmol) in DMF (0.5 mL). The suspension was stirred overnight at room temperature. The reaction mixture was diluted with water (20 mL) and extracted with ethyl acetate (3 \times 20 mL). The combined organic extracts were dried over sodium sulfate, filtered, and concentrated in vacuo. The residue was purified by silica gel chromatography (gradient, 0–100% ethyl acetate in heptanes) to provide **12d** as a white solid (18 mg, 42%). 1H NMR (500 MHz $CDCl_3$) δ 1.10–1.19 (br s, 3H), 1.32 (d, $J = 6.1$ Hz, 6H), 1.71–1.81 (m, 1H), 1.98–2.10 (m, 1H), 2.12–2.25 (m, 1H), 2.33–2.40 (m, 1H), 2.59–2.67 (m, 1H), 2.76–2.86 (m, 1H), 3.29–3.40 (m, 1H), 3.66–3.74 (m, 1H), 3.84 (d, $J = 8.5$ Hz, 1H), 3.93 (d, $J = 8.5$ Hz, 1H), 4.48–4.55 (m, 1H), 6.72–6.83 (m, 3H), 7.10–7.25 (m, 6H), 7.4–7.47 (m, 1H), 8.54 (d, $J = 5.9$ Hz, 2H). ^{13}C NMR ($CDCl_3$) δ 16.35, 22.23, 22.25, 33.81, 41.97, 44.90, 51.36, 56.26, 57.94, 61.46, 69.90, 110.93(2), 114.29, 116.63, 117.55, 120.58, 121.04, 129.09, 129.41, 130.68, 134.22, 14005, 144.97, 150.99(2), 158.12, 161.61. HRMS [$M + H$]⁺ calcd for $C_{28}H_{34}N_4O_3FS$ 525.2330, found 525.2318.

(SR,7S)-1-(3-Fluorophenyl)-8-(3-isopropoxybenzyl)-7-methyl-3-(pyrimidin-2-yl)-2-thia-1,3,8-triazaspiro[4.5]decane 2,2-Dioxide (12f). Application of the procedure used to make **12d**, using 2-bromopyrimidine in place of 4-bromopyridine hydrochloride, afforded benzyl (SR,7S)-1-(3-fluorophenyl)-7-methyl-3-(pyrimidin-2-yl)-2-thia-1,3,8-triazaspiro[4.5]decane-8-carboxylate 2,2-dioxide as a white solid (36.7 mg, 52%). 1H NMR (500 MHz, $CDCl_3$) δ 8.62 (d, $J = 4.9$ Hz, 2H), 7.43–7.49 (m, 1H), 7.26–7.38 (m, 6H), 7.18–7.26 (m, 2H), 7.03 (t, $J = 4.9$ Hz, 1H), 5.08 (br s, 2H), 4.59 (br s, 1H), 4.54 (d, $J = 10.0$ Hz, 1H), 4.21 (br s, 1H), 4.16 (d, $J = 10.0$ Hz, 1H), 3.12 (t, $J = 13.4$ Hz, 1H), 2.26 (d, $J = 12.9$ Hz, 1H), 1.72–1.86 (m, 3H), 1.31 (d, $J = 7.3$ Hz, 3H). MS (ESI) m/z : 512.1 ($M + 1$).

Application of the procedure used to make **12d**, employing (SR,7S)-1-(3-fluorophenyl)-7-methyl-3-(pyrimidin-2-yl)-2-thia-1,3,8-triazaspiro[4.5]decane 2,2-dioxide, afforded **12f** as a white solid (10 mg, 40%). 1H NMR (500 MHz, $CDCl_3$) δ 1.03–1.14 (br s, 3H), 1.28 (d, $J = 6.1$ Hz, 6H), 1.61–1.71 (m, 1H), 1.92–2.02 (m, 1H), 2.04–2.16 (m, 2H), 2.29–2.38 (br s, 1H), 2.53–2.63 (m, 1H), 2.73–2.83 (br s, 1H),

3.30 (d, $J = 13.3$ Hz, 1H), 3.62 (d, $J = 14.3$ Hz, 1H), 4.02 (d, $J = 9.6$ Hz, 1H), 4.27 (d, $J = 9.9$ Hz, 1H), 4.42–4.53 (m, 1H), 6.69–6.78 (m, 3H), 6.96 (t, $J = 4.9$ Hz, 1H), 7.10–7.19 (m, 2H), 7.20–7.28 (m, 1H, assumed, partially obscured by solvent peak), 7.33–7.42 (m, 2H), 8.57 (d, $J = 4.9$ Hz, 2H); ^{13}C NMR (CDCl_3) δ 16.15, 22.22, 22.25, 33.45, 41.52, 44.84, 51.47, 56.18, 57.96, 60.92, 69.90, 114.34, 115.68, 116.65, 117.18, 120.67, 121.06, 129.17, 129.39, 130.44, 134.84, 140.35, 157.28, 158.12, 158.56 (2), 161.56. HRMS $[\text{M} + \text{H}]^+$ calcd for $\text{C}_{27}\text{H}_{33}\text{N}_3\text{O}_3\text{FS}$ 526.2282, found 526.2275.

***N*-(4-[(*S*,*R*)-1-(3-Fluorophenyl)-3,7-dimethyl-2,2-dioxido-2-thia-1,3,8-triazaspiro[4.5]dec-8-yl)methyl]phenyl)acetamide (14a).** To a solution of (*S*,*R*)-1-(3-fluorophenyl)-3,7-dimethyl-2-thia-1,3,8-triazaspiro[4.5]decane 2,2-dioxide (20 mg, 0.064 mmol) and *N*-(4-formylphenyl)acetamide (10.4 mg, 0.064 mmol) in dichloroethane (0.5 mL) was added acetic acid (3.8 mg, 0.064 mmol). The mixture was allowed to stir at room temperature for 5 h, then was charged with sodium triacetoxyborohydride (27.1 mg, 0.128 mmol) and stirred overnight. The reaction was quenched with aqueous NaHCO_3 solution, extracted with CH_2Cl_2 , dried over Na_2SO_4 , filtered, and concentrated. Purification by silica gel chromatography using 20–70% gradient of ethyl acetate/heptane provided the first eluent (15 mg, 47%) of the title compound 14a. MS (LCMS) m/z 461.3 ($\text{M} + 1$). ^1H NMR (400 MHz, CDCl_3) δ 1.01 (d, $J = 6.8$ Hz, 3H), 1.61 (dd, $J = 13.4, 5.4$ Hz, 1H), 1.87–1.92 (m, 1H), 2.00 (dd, $J = 13.5, 4.9$ Hz, 1H), 2.11 (s, 3H), 2.22–2.30 (m, 1H), 2.44–2.53 (m, 1H), 2.70–2.77 (m, 1H), 2.79 (s, 3H), 3.23 (d, $J = 9.2$ Hz, 1H), 3.29 (d, $J = 13.5$ Hz, 1H), 3.41 (d, $J = 9.2$ Hz, 1H), 3.45 (q, $J = 7.0$ Hz, 1H), 3.52 (d, $J = 13.5$ Hz, 1H), 7.05–7.17 (m, 5H), 7.26 (s, 1H), 7.31–7.39 (m, 3H). HRMS calcd for $\text{C}_{23}\text{H}_{29}\text{N}_4\text{O}_3\text{FS}$ ($\text{M} + 1$) 461.2026, found 461.2017.

(*S*,*R*)-1-(3-Fluorophenyl)-8-(1*H*-indol-5-ylmethyl)-3,7-dimethyl-2-thia-1,3,8-triazaspiro[4.5]decane 2,2-Dioxide (14b). To a solution of (*S*,*R*)-1-(3-fluorophenyl)-3,7-dimethyl-2-thia-1,3,8-triazaspiro[4.5]decane 2,2-dioxide (18 mg, 0.057 mmol) and 1*H*-indole-5-carbaldehyde (12.5 mg, 0.086 mmol) in dichloroethane (0.5 mL) was added acetic acid (3.4 mg, 0.057 mmol). The mixture was allowed to stir at room temperature for 5 h, then was charged with sodium triacetoxyborohydride (24.2 mg, 0.114 mmol) and stirred overnight. The reaction was quenched with aqueous NaHCO_3 solution, extracted with CH_2Cl_2 , dried over Na_2SO_4 , filtered, and concentrated. Purification by silica gel chromatography using 20–100% gradient of ethyl acetate/heptane provided the first eluent (16 mg, 59%) of the title compound 14b. MS (LCMS) m/z 443.5 ($\text{M} + 1$). ^1H NMR (400 MHz, CDCl_3) δ 1.07 (d, $J = 6.6$ Hz, 3H), 1.57–1.66 (m, 1H), 1.86–1.95 (m, 2H), 1.99–2.09 (m, 1H), 2.26–2.39 (m, 1H), 2.48–2.59 (m, 1H), 2.74–2.78 (m, 1H), 2.79 (s, 3H), 3.22 (d, $J = 9.4$ Hz, 1H), 3.39 (d, $J = 9.2$ Hz, 1H), 3.42–3.48 (m, 1H), 3.69 (d, $J = 13.1$ Hz, 1H), 6.44–6.48 (m, 1H), 6.51–6.55 (m, 1H), 6.99–7.30 (m, 4H), 7.33–7.43 (m, 2H), 7.62 (d, $J = 0.8$ Hz, 1H), 8.22 (br s, 1H). HRMS calcd for $\text{C}_{23}\text{H}_{27}\text{N}_4\text{O}_2\text{FS}$ ($\text{M} + 1$) 443.1916, found 443.1911.

(*S*,*R*)-8-[(3-Ethyl-1*H*-indazol-5-yl)methyl]-1-(3-fluorophenyl)-3,7-dimethyl-2-thia-1,3,8-triazaspiro[4.5]decane 2,2-Dioxide (14c). To a solution of (*S*,*R*)-1-(3-fluorophenyl)-3,7-dimethyl-2-thia-1,3,8-triazaspiro[4.5]decane 2,2-dioxide (20 mg, 0.064 mmol) and 3-ethyl-1*H*-indazole-5-carbaldehyde⁴³ (22.3 mg, 0.128 mmol) in dichloroethane (0.5 mL) was added acetic acid (3.8 mg, 0.063 mmol). The mixture was allowed to stir at room temperature for 5 h, then was charged with sodium triacetoxyborohydride (27.1 mg, 0.128 mmol) and stirred overnight. The reaction was quenched with aqueous NaHCO_3 solution, extracted with CH_2Cl_2 , dried over Na_2SO_4 , filtered, and concentrated. Purification by silica gel chromatography using 0–50% gradient of acetone/ethyl acetate provided the first eluent (6 mg, 20%) of the title compound 14c. MS (LCMS) m/z 472.5 ($\text{M} + 1$). ^1H NMR (400 MHz, CDCl_3) δ 1.11 (d, $J = 6.6$ Hz, 3H), 1.27 (t, $J = 7.1$ Hz, 3H), 1.64–1.71 (m, 1H), 2.06 (s, 3H), 2.32–2.37 (m, 1H), 2.55–2.62 (m, 1H), 2.79–2.82 (m, 1H), 2.83 (s, 3H), 3.01–3.06 (q, 2H), 3.28 (d, $J = 9.3$ Hz, 1H), 3.44–3.50 (m, 2H), 3.73 (d, $J = 13.7$ Hz, 1H), 4.82 (s, 3H), 7.09–7.15 (m, 2H), 7.19 (d, $J = 8.5$ Hz, 1H), 7.31–7.36 (m, 2H), 7.40–7.46 (m, 2H), 7.48 (s, 1H), 7.72 (s, 1H). HRMS calcd for $\text{C}_{24}\text{H}_{30}\text{N}_5\text{O}_2\text{FS}$ ($\text{M} + 1$) 472.2177, found 472.2172.

4-[(*S*,*R*)-1-(3-Fluorophenyl)-3,7-dimethyl-2,2-dioxido-2-thia-1,3,8-triazaspiro[4.5]dec-8-yl)methyl]phenol (14d). To a solution of (*S*,*R*)-1-(3-fluorophenyl)-3,7-dimethyl-2-thia-1,3,8-triazaspiro[4.5]decane 2,2-dioxide (20 mg, 0.064 mmol) and 4-hydroxybenzaldehyde (11.7 mg, 0.096 mmol) in dichloroethane (0.5 mL) was added acetic acid (3.8 mg, 0.064 mmol). The mixture was allowed to stir at room temperature for 5 h, then was charged with sodium triacetoxyborohydride (27.1 mg, 0.128 mmol) and stirred overnight. The reaction was quenched with aqueous NaHCO_3 solution, extracted with CH_2Cl_2 , dried over Na_2SO_4 , filtered, and concentrated. Purification by silica gel chromatography using 20–70% gradient of ethyl acetate/heptane provided the first eluent (20.9 mg, 54%) of the title compound 14d. MS (LCMS) m/z 420.1 ($\text{M} + 1$). ^1H NMR (400 MHz, CDCl_3) δ 1.07 (d, $J = 6.6$ Hz, 3H), 1.66 (dd, $J = 14.3, 5.7$ Hz, 1H), 1.92–1.99 (m, 2H), 2.02–2.10 (m, 1H), 2.29–2.36 (m, 1H), 2.48–2.58 (m, 1H), 2.74–2.81 (m, 1H), 2.83 (s, 3H), 3.27 (d, $J = 9.3$ Hz, 1H), 3.33 (d, $J = 13.2$ Hz, 1H), 3.44 (d, $J = 9.3$ Hz, 1H), 3.55 (d, $J = 13.4$ Hz, 1H), 5.10 (br s, 1H), 6.72 (d, $J = 8.5$ Hz, 2H), 7.05 (d, $J = 8.3$ Hz, 2H), 7.10–7.15 (m, 1H), 7.15–7.21 (m, 2H), 7.34–7.43 (m, 1H). HRMS calcd for $\text{C}_{21}\text{H}_{26}\text{N}_3\text{O}_3\text{FS}$ ($\text{M} + 1$) 420.1756, found 420.1751.

2-Chloro-4-[(*S*,*R*)-1-(3-fluorophenyl)-3,7-dimethyl-2,2-dioxido-2-thia-1,3,8-triazaspiro[4.5]dec-8-yl)methyl]phenol (14e). To a solution of (*S*,*R*)-1-(3-fluorophenyl)-3,7-dimethyl-2-thia-1,3,8-triazaspiro[4.5]decane 2,2-dioxide (27 mg, 0.086 mmol) and 3-chloro-4-hydroxybenzaldehyde (15.5 mg, 0.086 mmol) in dichloroethane (0.5 mL) was added acetic acid (5.2 mg, 0.086 mmol). The mixture was allowed to stir at room temperature for 5 h, then was charged with sodium triacetoxyborohydride (36.5 mg, 0.172 mmol) and stirred overnight. The reaction was quenched with aqueous NaHCO_3 solution, extracted with CH_2Cl_2 , dried over Na_2SO_4 , filtered, and concentrated. Purification by silica gel chromatography using 0–5% gradient of $\text{MeOH}/\text{CH}_2\text{Cl}_2$ provided the first eluent (29.9 mg, 68%) of the title compound 14e. MS (LCMS) m/z 454.2 ($\text{M} + 1$). ^1H NMR (400 MHz, CDCl_3) δ 1.04 (d, $J = 6.6$ Hz, 3H), 1.24–1.32 (m, 2H), 1.64 (dd, $J = 13.7, 5.4$ Hz, 1H), 1.89–1.97 (m, 1H), 2.05 (dd, $J = 13.5, 4.8$ Hz, 1H), 2.22–2.33 (m, 1H), 2.44–2.56 (m, 1H), 2.71–2.79 (m, 1H), 2.82 (s, 3H), 3.22–3.31 (m, 2H), 3.43 (d, $J = 9.5$ Hz, 1H), 3.47–3.54 (m, 1H), 5.51 (br s, 1H), 6.87–6.93 (m, 1H), 6.96–7.02 (m, 1H), 7.10–7.21 (m, 4H), 7.34–7.43 (m, 1H). HRMS calcd for $\text{C}_{21}\text{H}_{25}\text{N}_3\text{O}_3\text{FCl}$ ($\text{M} + 1$) 454.1361, found 454.1357.

2-Ethoxy-4-[(*S*,*R*)-1-(3-fluorophenyl)-3,7-dimethyl-2,2-dioxido-2-thia-1,3,8-triazaspiro[4.5]dec-8-yl)methyl]phenol (14f). To a solution of (*S*,*R*)-1-(3-fluorophenyl)-3,7-dimethyl-2-thia-1,3,8-triazaspiro[4.5]decane 2,2-dioxide (25 mg, 0.08 mmol) and 3-ethoxy-4-hydroxybenzaldehyde (13.3 mg, 0.08 mmol) in dichloroethane (0.5 mL) was added acetic acid (4.8 mg, 0.08 mmol). The mixture was allowed to stir at room temperature for 5 h, then was charged with sodium triacetoxyborohydride (33.9 mg, 0.160 mmol) and stirred overnight. The reaction was quenched with aqueous NaHCO_3 solution, extracted with CH_2Cl_2 , dried over Na_2SO_4 , filtered, and concentrated. Purification by silica gel chromatography using a 0–4% gradient of $\text{MeOH}/\text{CH}_2\text{Cl}_2$ provided the first eluent (9.7 mg, 24%) of the title compound 14f. MS (LCMS) m/z 464.3 ($\text{M} + 1$). ^1H NMR (400 MHz, CDCl_3) δ 1.01 (d, $J = 6.8$ Hz, 3H), 1.38 (t, $J = 7.0$ Hz, 3H), 1.61 (dd, $J = 13.6, 5.4$ Hz, 1H), 1.87–1.93 (m, 2H), 2.00 (dd, $J = 13.7, 4.9$ Hz, 1H), 2.23–2.32 (m, 1H), 2.44–2.53 (m, 1H), 2.72–2.78 (m, 1H), 2.79 (s, 3H), 3.22 (d, $J = 9.4$ Hz, 1H), 3.26 (d, $J = 13.3$ Hz, 1H), 3.41 (d, $J = 9.2$ Hz, 1H), 3.44–3.50 (m, 1H), 4.01 (q, $J = 7.0$ Hz, 1H), 5.58 (br s, 1H), 6.62 (dd, $J = 8.0, 2.0$ Hz, 1H), 6.66 (d, $J = 1.8$ Hz, 1H), 6.77 (d, $J = 8.0$ Hz, 1H), 7.07–7.18 (m, 3H), 7.31–7.39 (m, 1H). HRMS calcd for $\text{C}_{23}\text{H}_{30}\text{N}_3\text{O}_4\text{FS}$ ($\text{M} + 1$) 464.2008, found 464.2013.

4-[(*S*,*R*)-1-(3-Fluorophenyl)-3,7-dimethyl-2,2-dioxido-2-thia-1,3,8-triazaspiro[4.5]dec-8-yl)methyl]-2-isopropoxyphenol (14g). To a solution of (*S*,*R*)-1-(3-fluorophenyl)-3,7-dimethyl-2-thia-1,3,8-triazaspiro[4.5]decane 2,2-dioxide (27 mg, 0.086 mmol) and 4-hydroxy-3-isopropoxybenzaldehyde⁴⁴ (15.5 mg, 0.086 mmol) in dichloroethane (0.5 mL) was added acetic acid (5.2 mg, 0.086 mmol). The mixture was allowed to stir at room temperature for 5 h, then was

charged with sodium triacetoxyborohydride (36.5 mg, 0.172 mmol) and stirred overnight. The reaction was quenched with aqueous NaHCO₃ solution, extracted with CH₂Cl₂, dried over Na₂SO₄, filtered, and concentrated. Purification by silica gel chromatography using 0–5% gradient of methanol/dichloromethane provided the first eluent (29.9 mg, 68%) of the title compound **14g**. MS (LCMS) *m/z* 464.3 (*M* + 1). ¹H NMR (400 MHz, CD₃OD) δ 7.41 (dt, *J* = 6.63, 8.2 Hz, 1H), 7.11–7.28 (m, 3H), 6.69–6.80 (m, 2H), 6.62 (dd, *J* = 1.0, 8.2 Hz, 1H), 4.43–4.58 (m, 1H), 3.49–3.62 (m, 2H), 3.38–3.49 (m, 1H), 3.28–3.33 (m, 1H), 2.80 (s, 3H), 2.54–2.71 (m, 2H), 2.23–2.38 (m, 1H), 2.05–2.18 (m, 2H), 1.86–2.00 (m, 1H), 1.68 (dd, *J* = 7.4, 13.7 Hz, 1H), 1.32 (dd, *J* = 1.4, 6.0 Hz, 6H), 1.14 (d, *J* = 6.6 Hz, 3H). ¹³C NMR (100 MHz, CD₃OD) δ 163.8, 161.3, 146.8, 145.2, 135.2, 130.1, 129.2, 122.3, 120.1, 119.9, 116.1, 116.3, 114.8, 71.2, 61.4, 60.4, 56.6, 50.5, 44.4, 41.7, 33.9, 31.8, 20.9, 15.3. HRMS calcd for C₂₄H₃₃N₃O₄FS (*M* + 1) 478.2162, found 478.2170.

Computational Details. The crystal structure for BACE-1 complexed with inhibitor **12a** was employed in the WaterMap calculation. The complex was prepared with the Protein Preparation Wizard in Maestro (version 9.2, Schrödinger, LLC, New York, NY, 2011), where it was submitted to a series of restrained, partial minimizations using the OPLS-AA force field.⁴⁵ Ligands were generated with LigPrep (version 2.5, Schrödinger, LLC, New York, NY, 2011) and their cores superimposed to the one from compound **12a**, followed by conformational search for the R groups and energy minimization using eMBrAcE (within MacroModel, version 9.9, Schrödinger, LLC, New York, NY, 2011). WaterMap was run in the default mode using the crystal structure ligand to define the binding site but removed in the MD simulation. The poses obtained for the ligands with the eMBrAcE procedure were scored using the ab initio form of the displaced-solvent functional as described by Abel and co-workers that estimates the free energy of liberation (ΔG_{WM}).²¹

■ ASSOCIATED CONTENT

● Supporting Information

Exposure data from in vivo mouse experiments, the Cerep profile of lead compound **14g**, spectral data for **12a** and **14g**, and the WaterMap entropy, enthalpy, and free energy liberation of binding site waters for analogues in Table 1. This material is available free of charge via the Internet at <http://pubs.acs.org>.

Accession Codes

Atomic coordinates and structure factors for the following BACE cocrystal structures have been deposited with the RCSB: compound **12a** (PDB code 4FM8) and compound **14g** (PDB code 4FM7).

■ AUTHOR INFORMATION

Corresponding Author

*Phone: 617 395 0706. E-mail: michael.a.brodney@pfizer.com.

Notes

The authors declare no competing financial interest.

■ ACKNOWLEDGMENTS

The authors thank Luis Martinez-Alsina for synthetic expertise, and Dan Virtue and Bob Depianta for chiral HPLC separations. We also gratefully acknowledge Christopher Butler, Jennifer Davoren, Shawn Doran, and Yasong Lu for helpful discussion of the manuscript.

■ REFERENCES

- (1) Hardy, J.; Allsop, D. Amyloid deposition as the central event in the aetiology of Alzheimer's disease. *Trends Pharmacol. Sci.* **1991**, *12* (10), 383–388.
- (2) Tanzi, R. E.; Bertram, L. Twenty years of the Alzheimer's disease amyloid hypothesis: a genetic perspective. *Cell* **2005**, *120* (4), 545–555.

- (3) De Strooper, B. Proteases and proteolysis in Alzheimer disease: a multifactorial view on the disease process. *Physiol. Rev.* **2010**, *90* (2), 465–494.

- (4) Vassar, R.; Kovacs, D. M.; Yan, R.; Wong, P. C. The beta-secretase enzyme BACE in health and Alzheimer's disease: regulation, cell biology, function, and therapeutic potential. *J. Neurosci.* **2009**, *29* (41), 12787–12794.

- (5) Marks, N.; Berg, M. J. BACE and gamma-secretase characterization and their sorting as therapeutic targets to reduce amyloidogenesis. *Neurochem. Res.* **2010**, *35* (2), 181–210.

- (6) Stachel, S. J. Progress toward the development of a viable BACE-1 inhibitor. *Drug Dev. Res.* **2009**, *70* (2), 101–110.

- (7) Didziapetris, R.; Japertas, P.; Avdeef, A.; Petrauskas, A. Classification analysis of P-glycoprotein substrate specificity. *J. Drug Targeting* **2003**, *11* (7), 391–406.

- (8) Gleeson, M. P. Generation of a set of simple, interpretable ADMET rules of thumb. *J. Med. Chem.* **2008**, *51* (4), 817–834.

- (9) Hitchcock, S. A.; Pennington, L. D. Structure–brain exposure relationships. *J. Med. Chem.* **2006**, *49* (26), 7559–7583.

- (10) Leeson, P. D.; Springthorpe, B. The influence of drug-like concepts on decision-making in medicinal chemistry. *Nat. Rev. Drug Discovery* **2007**, *6* (11), 881–890.

- (11) Wager, T. T.; Chandrasekaran, R. Y.; Hou, X.; Troutman, M. D.; Verhoest, P. R.; Villalobos, A.; Will, Y. Defining desirable central nervous system drug space through the alignment of molecular properties, in vitro ADME, and safety attributes. *ACS Chem. Neurosci.* **2010**, *1* (6), 420–434.

- (12) Cole, D. C.; Manas, E. S.; Stock, J. R.; Condon, J. S.; Jennings, L. D.; Aulabaugh, A.; Chopra, R.; Cowling, R.; Ellingboe, J. W.; Fan, K. Y.; Harrison, B. L.; Hu, Y.; Jacobsen, S.; Jin, G.; Lin, L.; Lovering, F. E.; Malamas, M. S.; Stahl, M. L.; Strand, J.; Sukhdeo, M. N.; Svenson, K.; Turner, M. J.; Wagner, E.; Wu, J.; Zhou, P.; Bard, J. Acylguanidines as small-molecule β -secretase inhibitors. *J. Med. Chem.* **2006**, *49* (21), 6158–6161.

- (13) Cole, D. C.; Stock, J. R.; Chopra, R.; Cowling, R.; Ellingboe, J. W.; Fan, K. Y.; Harrison, B. L.; Hu, Y.; Jacobsen, S.; Jennings, L. D.; Jin, G.; Lohse, P. A.; Malamas, M. S.; Manas, E. S.; Moore, W. J.; O'Donnell, M. M.; Olland, A. M.; Robichaud, A. J.; Svenson, K.; Wu, J.; Wagner, E.; Bard, J. Acylguanidine inhibitors of β -secretase: optimization of the pyrrole ring substituents extending into the S1 and S3 substrate binding pockets. *Bioorg. Med. Chem. Lett.* **2008**, *18* (3), 1063–1066.

- (14) Fobare, W. F.; Solvibile, W. R.; Robichaud, A. J.; Malamas, M. S.; Manas, E.; Turner, J.; Hu, Y.; Wagner, E.; Chopra, R.; Cowling, R.; Jin, G.; Bard, J. Thiophene substituted acylguanidines as BACE1 inhibitors. *Bioorg. Med. Chem. Lett.* **2007**, *17* (19), 5353–5356.

- (15) May, P. C.; Dean, R. A.; Lowe, S. L.; Martenyi, F.; Sheehan, S. M.; Boggs, L. N.; Monk, S. A.; Mathes, B. M.; Mergott, D. J.; Watson, B. M.; Stout, S. L.; Timm, D. E.; Smith Labell, E.; Gonzales, C. R.; Nakano, M.; Jhee, S. S.; Yen, M.; Ereshefsky, L.; Lindstrom, T. D.; Calligaro, D. O.; Cocke, P. J.; Greg Hall, D.; Friedrich, S.; Citron, M.; Audia, J. E. Robust central reduction of amyloid-beta in humans with an orally available, non-peptidic beta-secretase inhibitor. *J. Neurosci.* **2011**, *31* (46), 16507–16516.

- (16) Stachel, S. J.; Coburn, C. A.; Rush, D.; Jones, K. L.; Zhu, H.; Rajapakse, H.; Graham, S. L.; Simon, A.; Katharine Holloway, M.; Allison, T. J.; Munshi, S. K.; Espeseth, A. S.; Zuck, P.; Colussi, D.; Wolfe, A.; Pietrak, B. L.; Lai, M. T.; Vacca, J. P. Discovery of aminoheterocycles as a novel beta-secretase inhibitor class: pH dependence on binding activity part I. *Bioorg. Med. Chem. Lett.* **2009**, *19* (11), 2977–2980.

- (17) Barrow, J. C.; Stauffer, S. R.; Rittle, K. E.; Ngo, P. L.; Yang, Z.; Selnick, H. G.; Graham, S. L.; Munshi, S.; McGaughey, G. B.; Holloway, M. K.; Simon, A. J.; Price, E. A.; Sankaranarayanan, S.; Colussi, D.; Tugusheva, K.; Lai, M. T.; Espeseth, A. S.; Xu, M.; Huang, Q.; Wolfe, A.; Pietrak, B.; Zuck, P.; LeVorse, D. A.; Hazuda, D.; Vacca, J. P. Discovery and X-ray crystallographic analysis of a spiroperidine iminohydantoin inhibitor of β -secretase. *J. Med. Chem.* **2008**, *51* (20), 6259–6262.

- (18) Coburn, C. A.; Egbertson, M. S.; Graham, S. L.; McGaughey, G. B.; Stauffer, S. R.; Yang, W.; Lu, W.; Fahr, B. Preparation of 1,3,8-Triazaspiro[4.5]decane Derivatives as β -Secretase Inhibitors for Treatment of Alzheimer's Disease. *PCT Int. Appl. WO2007011810*, 2007.
- (19) Coburn, C. A.; Stachel, S. J.; Li, Y. M.; Rush, D. M.; Steele, T. G.; Chen-Dodson, E.; Holloway, M. K.; Xu, M.; Huang, Q.; Lai, M. T.; DiMuzio, J.; Crouthamel, M. C.; Shi, X. P.; Sardana, V.; Chen, Z.; Munshij, S.; Kuo, L.; Makara, G. M.; Annis, D. A.; Tadikonda, P. K.; Nash, H. M.; Vacca, J. P.; Wang, T. Identification of a small molecule nonpeptide active site beta-secretase inhibitor that displays a nontraditional binding mode for aspartyl proteases. *J. Med. Chem.* **2004**, *47* (25), 6117–6119.
- (20) Kuglstatler, A.; Stahl, M.; Peters, J. U.; Huber, W.; Stihle, M.; Schlatter, D.; Benz, J.; Ruf, A.; Roth, D.; Enderle, T.; Hennig, M. Tyramine fragment binding to BACE-1. *Bioorg. Med. Chem. Lett.* **2008**, *18* (4), 1304–1307.
- (21) Abel, R.; Young, T.; Farid, R.; Berne, B. J.; Friesner, R. A. Role of the active-site solvent in the thermodynamics of factor Xa ligand binding. *J. Am. Chem. Soc.* **2008**, *130* (9), 2817–2831.
- (22) Brodney, M. A.; Helal, C. J.; O'Neill, B. T. Preparation of Spiropiperidinethiadiazole Dioxides for the Treatment of Neurodegenerative Diseases. *PCT Int. Appl. WO2009136350*, 2009.
- (23) Henegar, K. E.; Lira, R. One-pot in situ formation and reaction of trimethyl(trichloromethyl)silane: application to the synthesis of 2,2,2-trichloromethylcarbinols. *J. Org. Chem.* **2012**, *77* (6), 2999–3004.
- (24) Sebesta, R.; Pizzuti, M. G.; Boersma, A. J.; Minnaard, A. J.; Feringa, B. L. Catalytic enantioselective conjugate addition of dialkylzinc reagents to N-substituted-2,3-dehydro-4-piperidones. *Chem. Commun. (Cambridge, U. K.)* **2005**, *13*, 1711–1713.
- (25) Beaudoin, S.; Kinsey, K. E.; Burns, J. F. Preparation of unsymmetrical sulfonylureas from *N,N'*-sulfuryldiimidazoles. *J. Org. Chem.* **2003**, *68* (1), 115–119.
- (26) Klapars, A.; Huang, X.; Buchwald, S. L. A general and efficient copper catalyst for the amidation of aryl halides. *J. Am. Chem. Soc.* **2002**, *124* (25), 7421–7428.
- (27) Feng, B.; Mills, J. B.; Davidson, R. E.; Mireles, R. J.; Janiszewski, J. S.; Troutman, M. D.; de Moraes, S. M. In vitro P-glycoprotein assays to predict the in vivo interactions of P-glycoprotein with drugs in the central nervous system. *Drug Metab. Dispos.* **2008**, *36* (2), 268–275.
- (28) Callegari, E.; Malhotra, B.; Bungay, P. J.; Webster, R.; Fenner, K. S.; Kempshall, S.; LaPerle, J. L.; Michel, M. C.; Kay, G. G. A comprehensive non-clinical evaluation of the CNS penetration potential of antimuscarinic agents for the treatment of overactive bladder. *Br. J. Clin. Pharmacol.* **2011**, *72* (2), 235–246.
- (29) Kalvass, J. C.; Maurer, T. S. Influence of nonspecific brain and plasma binding on CNS exposure: implications for rational drug discovery. *Biopharm. Drug Dispos.* **2002**, *23* (8), 327–338.
- (30) Guimaraes, C. R.; Mathiowetz, A. M. Addressing limitations with the MM-GB/SA scoring procedure using the WaterMap method and free energy perturbation calculations. *J. Chem. Inf. Model.* **2010**, *50* (4), 547–559.
- (31) Hitchcock, S. A. Structural modifications that alter the P-glycoprotein efflux properties of compounds. *J. Med. Chem.* **2012**, *55* (11), 4877–4895.
- (32) Kuhn, B.; Mohr, P.; Stahl, M. Intramolecular hydrogen bonding in medicinal chemistry. *J. Med. Chem.* **2010**, *53* (6), 2601–2611.
- (33) Atwal, J. K.; Chen, Y.; Chiu, C.; Mortensen, D. L.; Meilandt, W. J.; Liu, Y.; Heise, C. E.; Hoyte, K.; Luk, W.; Lu, Y.; Peng, K.; Wu, P.; Rouge, L.; Zhang, Y.; Lazarus, R. A.; Scarce-Levie, K.; Wang, W.; Wu, Y.; Tessier-Lavigne, M.; Watts, R. J. A therapeutic antibody targeting BACE1 inhibits amyloid-beta production in vivo. *Sci. Transl. Med.* **2011**, *3* (84), 84ra43.
- (34) Schinkel, A. H.; Smit, J. J.; van Tellingen, O.; Beijnen, J. H.; Wagenaar, E.; van Deemter, L.; Mol, C. A.; van der Valk, M. A.; Robanus-Maandag, E. C.; te Riele, H. P.; et al. Disruption of the mouse *mdr1a* P-glycoprotein gene leads to a deficiency in the blood–brain barrier and to increased sensitivity to drugs. *Cell* **1994**, *77* (4), 491–502.
- (35) Stepan, A. F.; Subramanyam, C.; Efremov, I. V.; Dutra, J. K.; O'Sullivan, T. J.; DiRico, K. J.; McDonald, W. S.; Won, A.; Dorff, P. H.; Nolan, C. E.; Becker, S. L.; Pustilnik, L. R.; Riddell, D. R.; Kauffman, G. W.; Kormos, B. L.; Zhang, L.; Lu, Y.; Capetta, S. H.; Green, M. E.; Karki, K.; Sibley, E.; Atchison, K. P.; Hallgren, A. J.; Oborski, C. E.; Robshaw, A. E.; Sneed, B.; O'Donnell, C. J. Application of the bicyclo[1.1.1]pentane motif as a nonclassical phenyl ring bioisostere in the design of a potent and orally active gamma-secretase inhibitor. *J. Med. Chem.* **2012**, *55* (7), 3414–3424.
- (36) Tomasselli, A. G.; Paddock, D. J.; Emmons, T. L.; Mildner, A. M.; Leone, J. W.; Lull, J. M.; Cialdella, J. I.; Prince, D. B.; Fischer, H. D.; Heinrikson, R. L.; Benson, T. E. High yield expression of human BACE constructs in *Escherichia coli* for refolding, purification, and high resolution diffracting crystal forms. *Protein Pept. Lett.* **2008**, *15* (2), 131–143.
- (37) Pflugrath, J. W. The finer things in X-ray diffraction data collection. *Acta Crystallogr., Sect. D* **1999**, *55*, 1718–1725.
- (38) Kabsch, W. XDS. *Acta Crystallogr., Sect. D* **2010**, *66* (2), 125–132.
- (39) Collaborative Computational Project Number 4. The CCP4 suite: programs for protein crystallography. *Acta Crystallogr.* **1994**, *DS0*, 760–763.
- (40) Murshudov, G. N.; Vagin, A. A.; Dodson, E. J. Refinement of macromolecular structures by the maximum-likelihood method. *Acta Crystallogr.* **1997**, *DS3*, 240–255.
- (41) Emsley, P.; Cowtan, K. Coot: model-building tools for molecular graphics. *Acta Crystallogr., Sect. D: Biol. Crystallogr.* **2004**, *60*, 2126–2132.
- (42) Bricogne, G.; Blanc, E.; Brandl, M.; Flensburg, C.; Keller, P.; Paciorek, W.; Roversi, P.; Smart, O. S.; Vonrhein, C.; Womack, T. O. BUSTER, version 2.8.0; Global Phasing Ltd.: Cambridge, U.K., 2009.
- (43) Michels, M.; Follmann, M.; Vakalopoulos, A.; Zimmermann, K.; Teusch, N.; Lobell, M. Indazolyl-Substituted Dihydroisoxazolopyridines as c-Met Tyrosine Kinase Inhibitors and Their Preparation. *WO2011003604*, 2011.
- (44) Dabak, K. Pyridine and benzene templated potential peptidomimetics. *Turk. J. Chem.* **2002**, *26* (6), 955–963.
- (45) Jorgensen, W. L.; Tirado-Rives, J. The OPLS [optimized potentials for liquid simulations] potential functions for proteins, energy minimizations for crystals of cyclic peptides and crambin. *J. Am. Chem. Soc.* **1988**, *110* (6), 1657–1666.